Parity Violation in Hadronic Systems

Christopher Crawford, University of Kentucky
Nuclear Seminar, University of Virginia
Charlottesville, VA 2015-01-20

Outline

- Hadronic Parity Violation
  - Hadronic Weak Interaction (HWI) formalism
- NPDGamma Experiment
  - Setup, preliminary results
- n-^{3}He Experiment
  - Setup, status update

$$A_\gamma \approx \vec{s}_n \cdot \vec{k}_\gamma$$

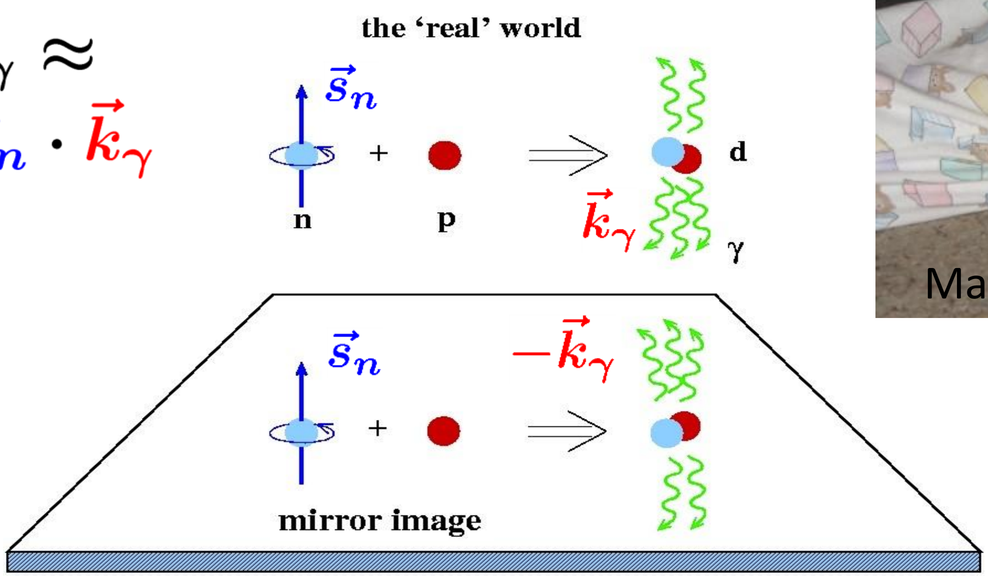

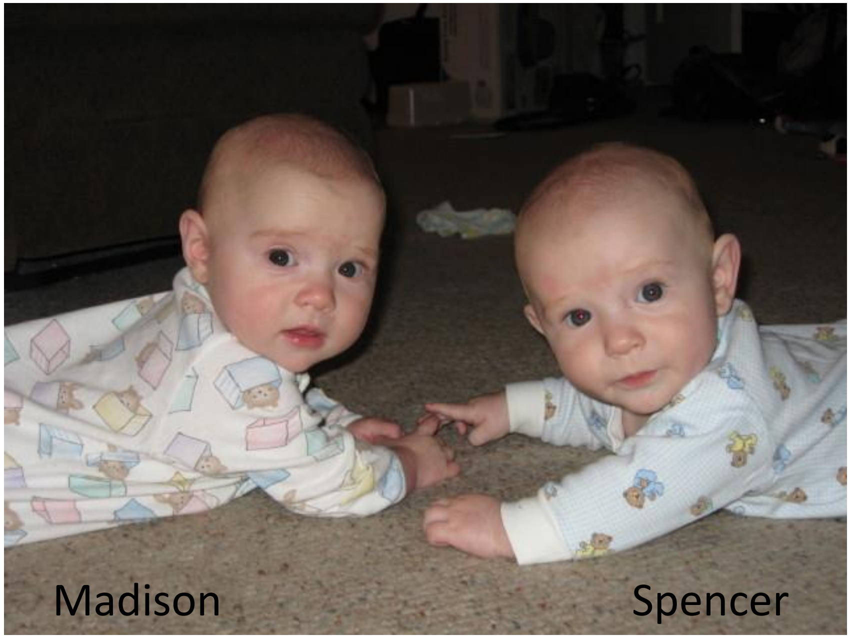

Hadronic Weak Interaction in a nutshell

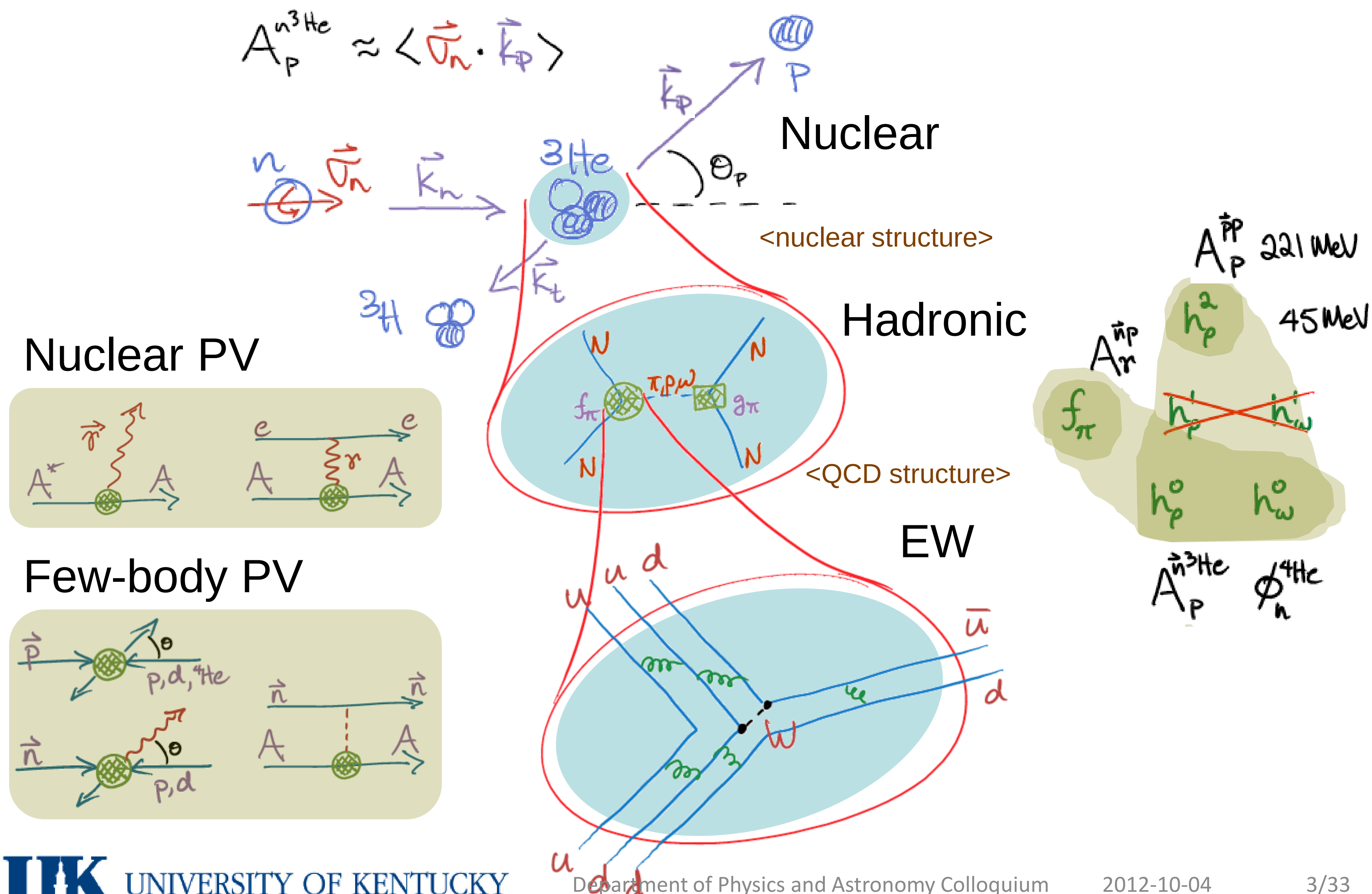

DDH Potential

PV meson exchange

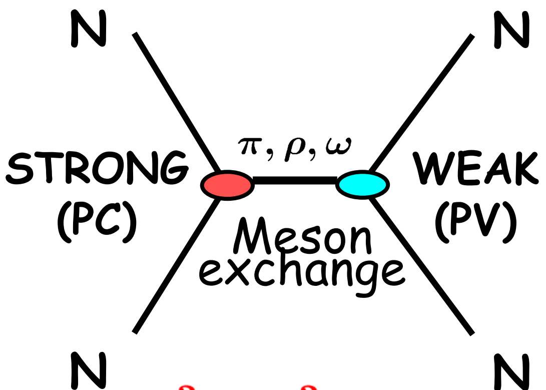

$$\frac{e^2}{M_W^2} \Big/ \frac{g^2}{m_\pi^2} \approx 10^{-7}$$

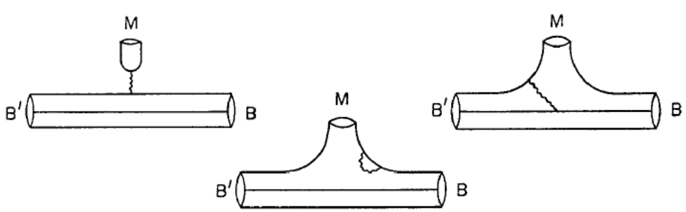

Desplanques, Donoghue, Holstein,
Annals of Physics 124, 449 (1980)

		f_π	$h_\rho'^{1}$	$h_\rho^{0,1,2}$	$h_\omega^{0,1}$
isospin	$\Delta I = 0$			$(\boldsymbol{\tau}_1 \cdot \boldsymbol{\tau}_2)$	(1)
	$\Delta I = 1$	$\frac{i}{2}(\boldsymbol{\tau}_1 \times \boldsymbol{\tau}_2)^3$		$\frac{1}{2}(\boldsymbol{\tau}_1 \pm \boldsymbol{\tau}_2)^3$	$\frac{1}{2}(\boldsymbol{\tau}_1 \pm \boldsymbol{\tau}_2)^3$
	$\Delta I = 2$			$\frac{1}{2\sqrt{6}}(3\tau_1^3\tau_2^3 - \boldsymbol{\tau}_1 \cdot \boldsymbol{\tau}_2)$	
		$J = 0$		$J = 1$	$J = 1$
range	m_π	$(\boldsymbol{\sigma}_1 + \boldsymbol{\sigma}_2)\left[\frac{\boldsymbol{p}_1 - \boldsymbol{p}_2}{2M}, \frac{e^{-m_\pi r}}{4\pi r}\right]$			
	$m_\rho = m_\omega$	$(\boldsymbol{\sigma}_1 + \boldsymbol{\sigma}_2)\left[\frac{\boldsymbol{p}_1 - \boldsymbol{p}_2}{2M}, \frac{e^{-m_\rho r}}{4\pi r}\right]$		$(\boldsymbol{\sigma}_1 \pm \boldsymbol{\sigma}_2)\left\{\frac{\boldsymbol{p}_1 - \boldsymbol{p}_2}{2M}, \frac{e^{-m_\rho r}}{4\pi r}\right\}$	
				$i(\boldsymbol{\sigma}_1 \times \boldsymbol{\sigma}_2)\left[\frac{\boldsymbol{p}_1 - \boldsymbol{p}_2}{2M}, \frac{e^{-m_\rho r}}{4\pi r}\right]$	

	np A_γ	nD A_γ	n^3He A_p	np ϕ	nα ϕ	pp A_z	pα A_z
f_π	-0.11	0.92	-0.18	-3.12	-0.97		-0.34
h_ρ^0		-0.50	-0.14	-0. 23	-0.32	0.08	0.14
h_ρ^1	-0.001	0.10	0.027		0.11	0.08	0.05
h_ρ^2		0.05	0.0012	-0.25		0.03	
h_ω^0		-0.16	-0.13	-0. 23	-0.22	-0.07	0.06
h_ω^1	-0.003	-0.002	0.05		0.22	0.07	0.06

Adelberger, Haxton, A.R.N.P.S. **35,** 501 (1985)

Danilov parameters / EFT

- Elastic NN scattering
  at low energy (<40 MeV)
  S-P transition (PV)

  S=1/2+1/2 ,   I=1/2+1/2

  Antisymmetric in L, S, I

  Conservation of   J

- Equivalent to Effective
  Field Theory (EFT)
  in low energy limit

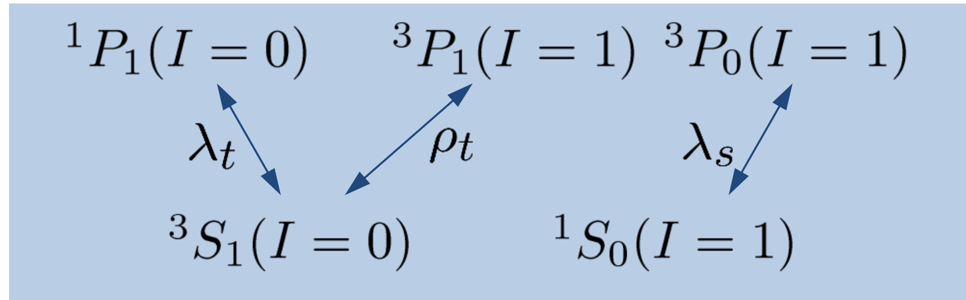

C.-P. Liu, PRC 75, 065501 (2007)

$$
\begin{aligned}
\lambda_t &\propto (C_1 - 3C_3) - (\tilde{C}_1 - 3\tilde{C}_3) \\
\lambda_s^0 &\propto (C_1 + C_3) + (\tilde{C}_1 + \tilde{C}_3) \\
\lambda_s^1 &\propto (C_2 + C_4) + (\tilde{C}_2 + \tilde{C}_4) \\
\lambda_s^2 &\propto -\sqrt{8/3}(C_5 + \tilde{C}_5) \\
\rho_t &\propto \frac{1}{2}(C_2 - C_4) + C_6 \quad .
\end{aligned}
$$

$$^3S_1 \longrightarrow {}^1P_1, \quad I = 0$$

$$^1S_0 \longrightarrow {}^3P_0, \quad I = 1$$

$$^3S_1 \longrightarrow {}^3P_1, \quad I = 1 \to 0$$

Existing HPV data

- p-p scat. 15, 45 MeV A_z^{pp}
- p-α scat. 46 MeV A_z^{pp}
- p-p scat. 220 MeV A_z^{pp}
- n+p→d+γ circ. pol. P_γ^{d}
- n+p→d+γ asym. A_γ^{d}
- n-α spin rot. $d\phi^{n\alpha}/dz$

Wasem, Phys. Rev. C **85** (2012) 022501

1st Lattice QCD result

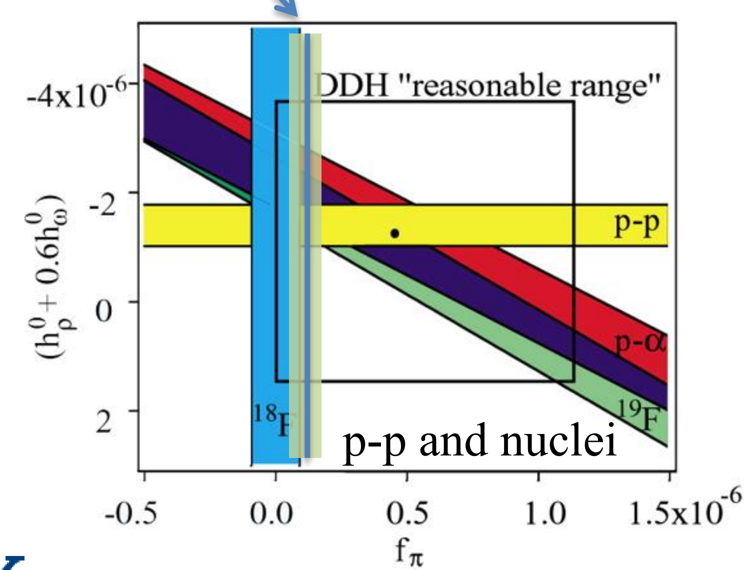

- ^{18}F asym. ΔI =1
- ^{19}F, ^{41}K, ^{175}Lu, ^{181}Ta asym.
- ^{21}Ne (even-odd)
- ^{133}Cs, ^{205}Tl anapole moment

GOAL – resolve coupling constants from few-body PV experiments only

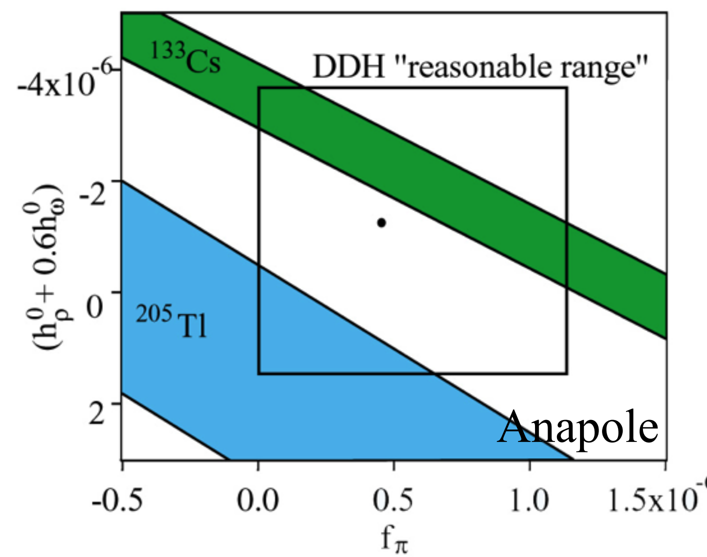

NPDGamma Collaboration

R. Alarcon[1], R. Allen[18], L.P. Alonzi[3], E. Askanazi[3], S. Baeßler[3], S. Balascuta[1], L. Barron-Palos[2], A. Barzilov[27], W. Berry[8], C. Blessinger[18], D. Blythe[1], D. Bowman[4], M. Bychkov[3], J. Calarco ,R. Carlini[5], W. Chen[6], T. Chupp[7], C. Crawford[8], M. Dabaghyan[9], A. Danagoulian[10], M. Dawkins[11], D. Evans[3], J. Favela[2], N. Fomin[12], W. Fox[11], E. Frlez[3], S. Freedman[13], J. Fry[11], C. Fu[11], C. Garcia[2], T. Gentile[6], M. Gericke[14] C. Gillis[11], K Grammer[12], G. Greene[4,12], J Hamblen[26], C. Hayes[12], F. Hersman[9], T. Ino[15], E. Iverson[4], G. Jones[16], K. Latiful[8], K. Kraycraft[8], S. Kucuker[12], B. Lauss[17], Y. Li[30], W. Lee[18], M. Leuschner[11], W. Losowski[11], R. Mahurin[12], M. Maldonado-Velazquez[2], E. Martin[8], Y. Masuda[15], M. McCrea[14], J. Mei[11], G. Mitchell[19], S. Muto[15], H. Nann[11], I. Novikov[25], S. Page[14], D. Parsons[26], S. Penttila[4], D. Pocinic[3], D. Ramsay[14,20], A. Salas-Bacci[3], S. Santra[21], S. Schroeder[3], P.-N. Seo[22], E. Sharapov[23], M. Sharma[7], T. Smith[24], W. Snow[11], J. Stuart[26], Z. Tang[11], J. Thomison[18], T. Tong[18], J. Vanderwerp[11], S. Waldecker[26], W. Wilburn[10], W. Xu[30], V. Yuan[10], Y. Zhang[29]

[1]Arizona State University
[2]Universidad Nacional Autonoma de Mexico
[3]University of Virginia
[4]Oak Ridge National Laboratory
[5]Thomas Jefferson National Laboratory
[6]National Institute of Standards and Technology
[7]Univeristy of Michigan, Ann Arbor
[8]University of Kentucky
[9]University of New Hampshire
[10]Los Alamos National Laboratory
[11]Indiana University
[12]University of Tennessee, Knoxville
[13]University of California at Berkeley
[14]University of Manitoba, Canada
[15]High Energy Accelerator Research Organization (KEK), Japan
[16]Hamilton College
[17]Paul Scherer Institute, Switzerland
[18]Spallation Neutron Source, ORNL
[19]University of California at Davis
[20]TRIUMF, Canada
[21]Bhabha Atomic Research Center, India
[22]Duke University
[23]Joint Institute of Nuclear Research, Dubna, Russia
[24]University of Dayton
[25]Western Kentucky University
[26]University of Tennessee at Chattanooga
[27]Univeristy of Nevada at Los Vegas
[28]University of California, Davis
[29]Lanzhou University
[30]Shanghai Institute of Applied Physics

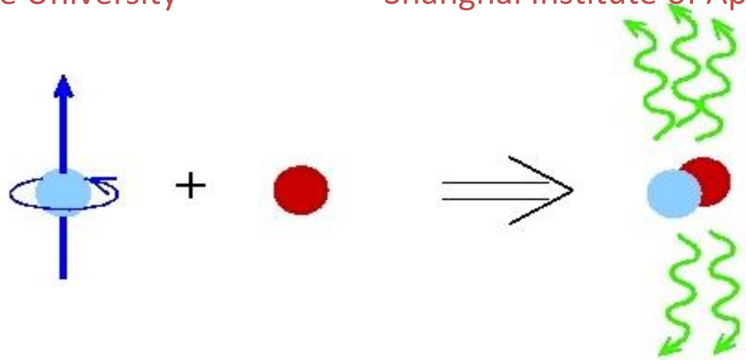

Experimental Layout

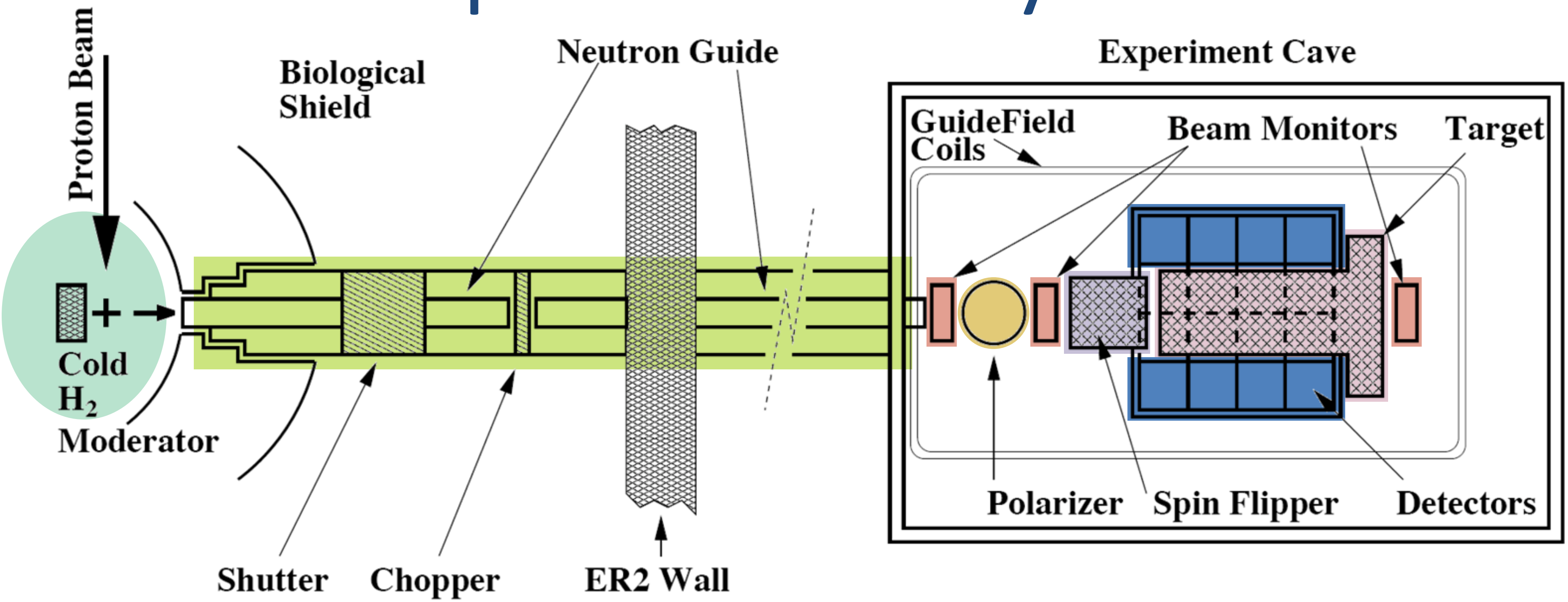

Supermirror Polarizer

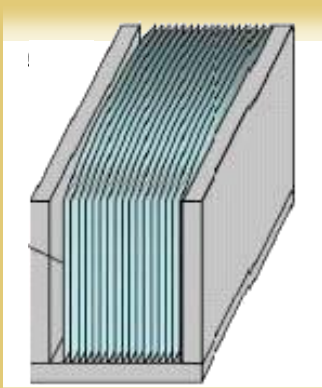

Beam Monitors

RF Spin Rotator

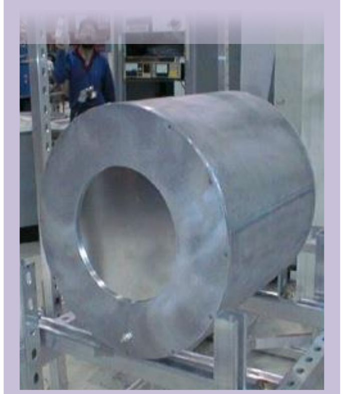

LH_2 Target

Gamma Detectors

Spallation neutron source

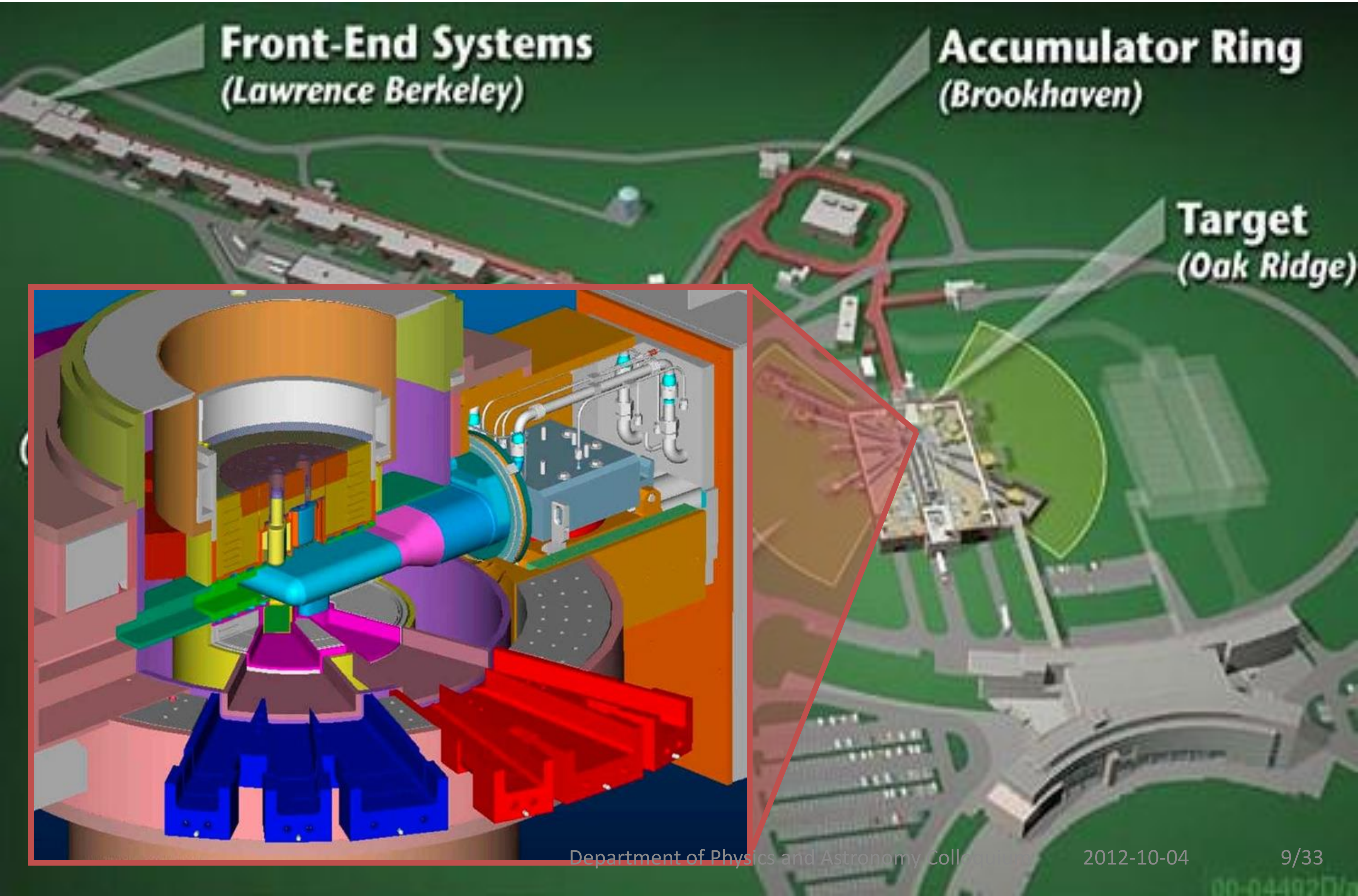

Neutron Flux at the SNS FnPB

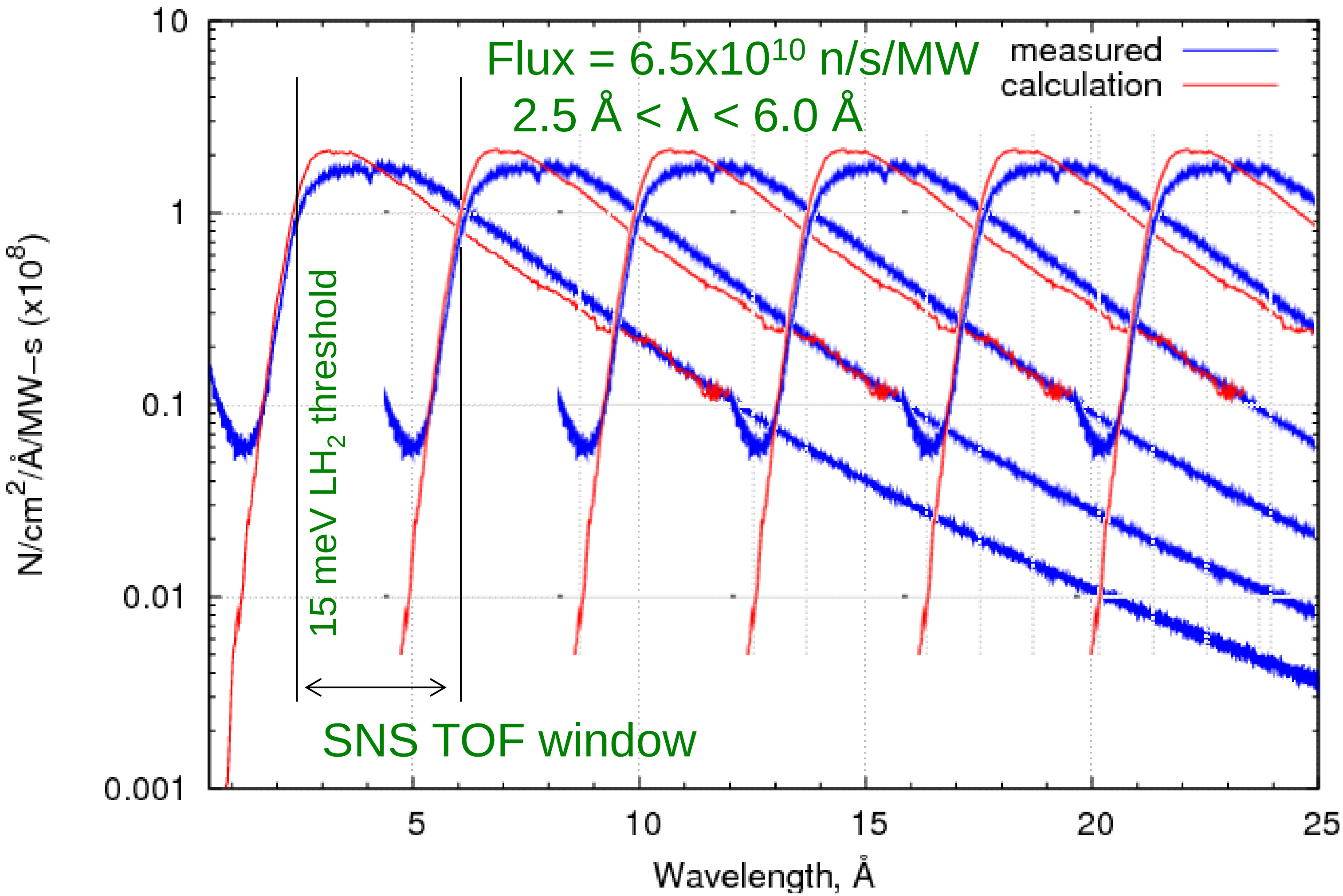

Chopped & folded spectrum

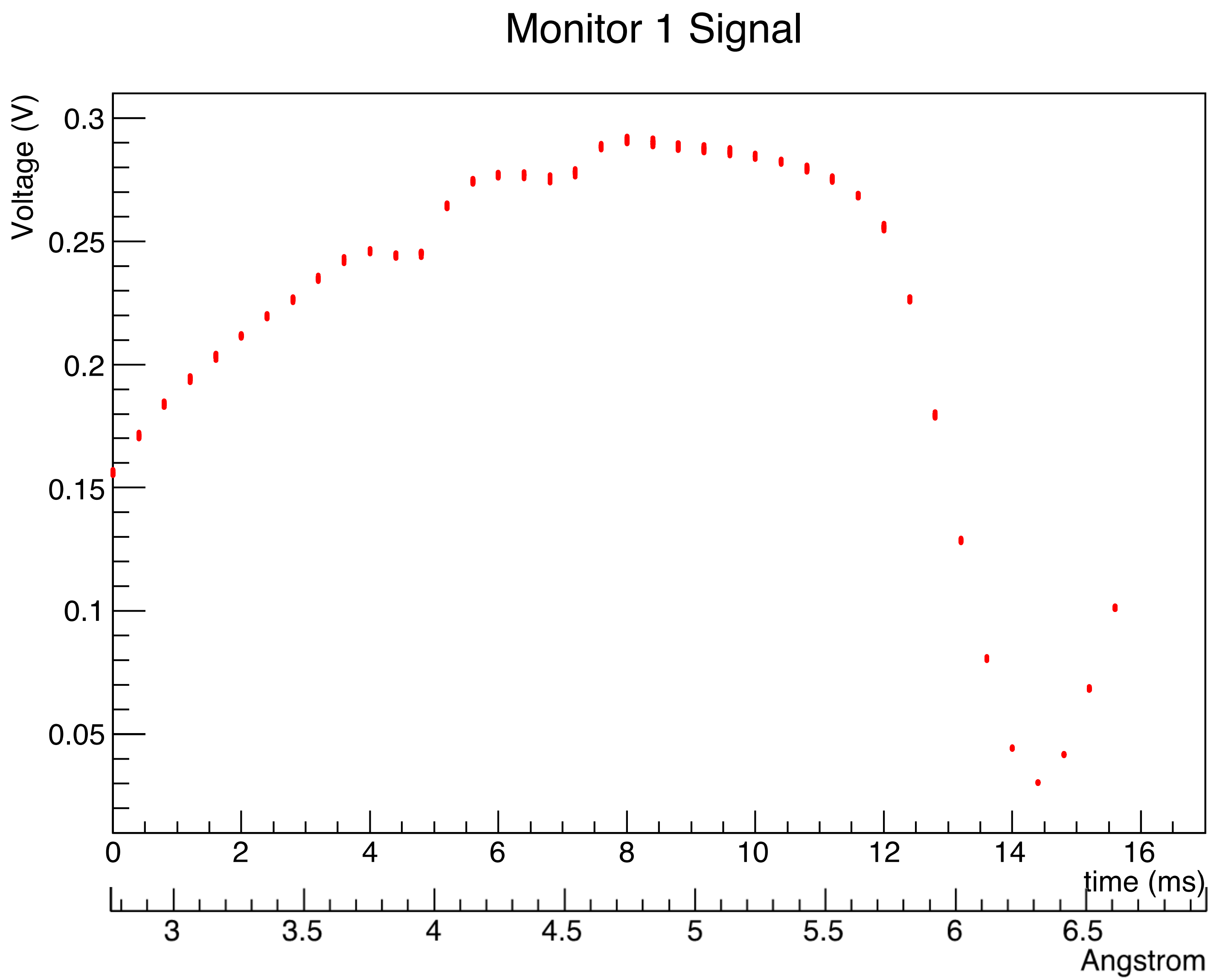

FnPB supermirror polarizer

T=25.8%	transmission
P=95.3%	polarization
N=2.2£10^{10} n/s	output flux (chopped)

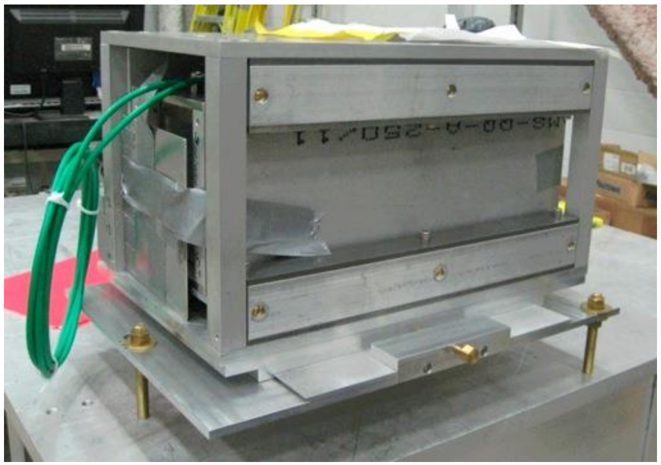

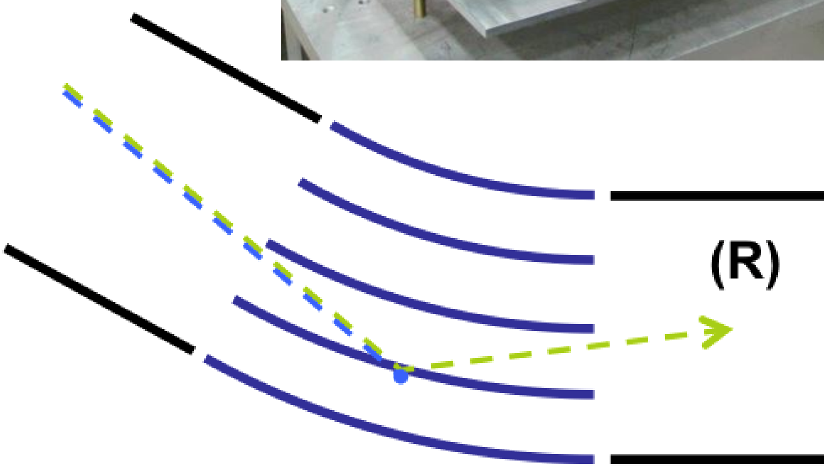

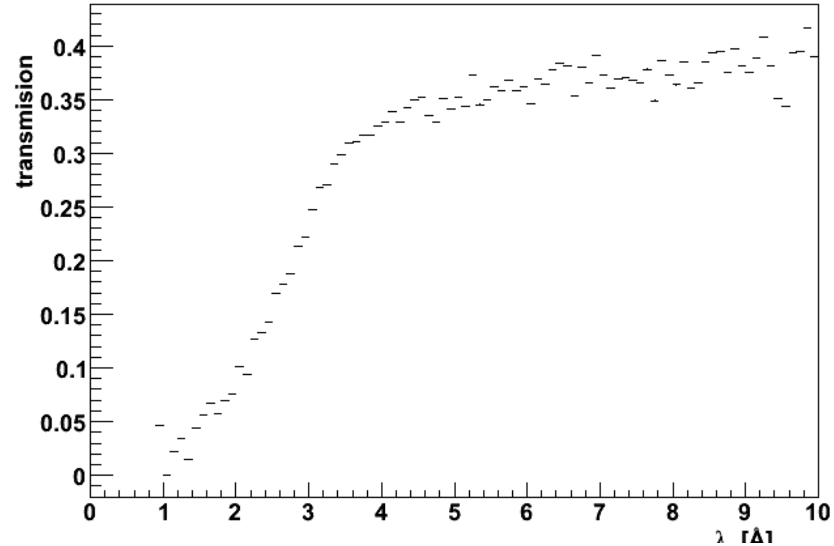

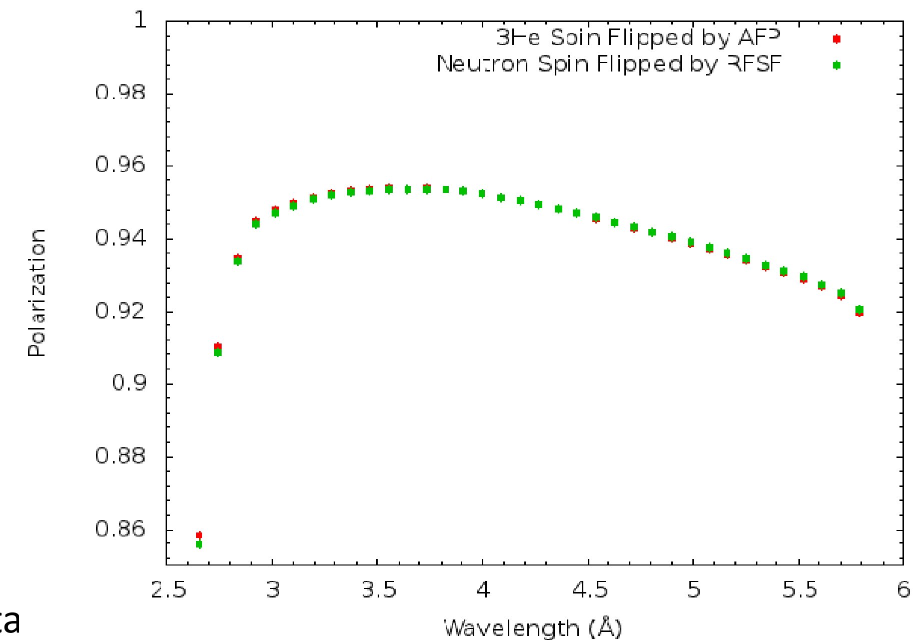

S. Balascuta

Longitudinal RF spin rotator

- Resonant RF spin rotator,
  - 1/t RF amplitude tuned to velocity of neutrons
  - Affects spin only – NOT velocity! (no static gradients)
- essential to reduce instrumental systematics
  - danger: must isolate RF field from the detector
  - false asymmetries: additive & multiplicave

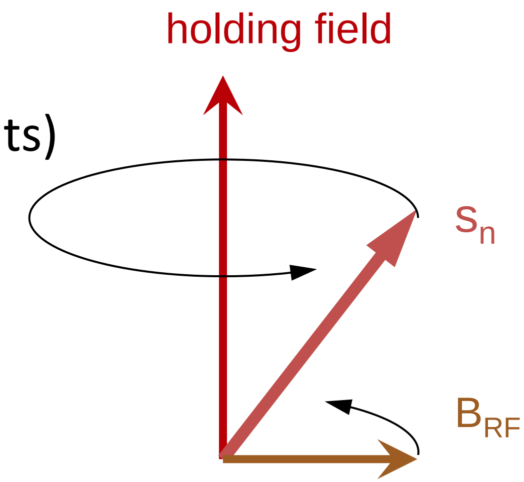

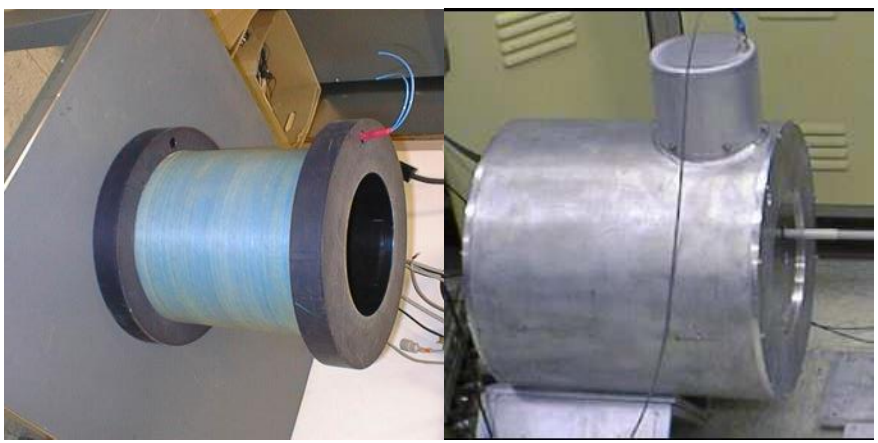

P. Neo-Seo, *et al.* Phys. Rev. ST Accel. Beams **11** 084701 (2008)

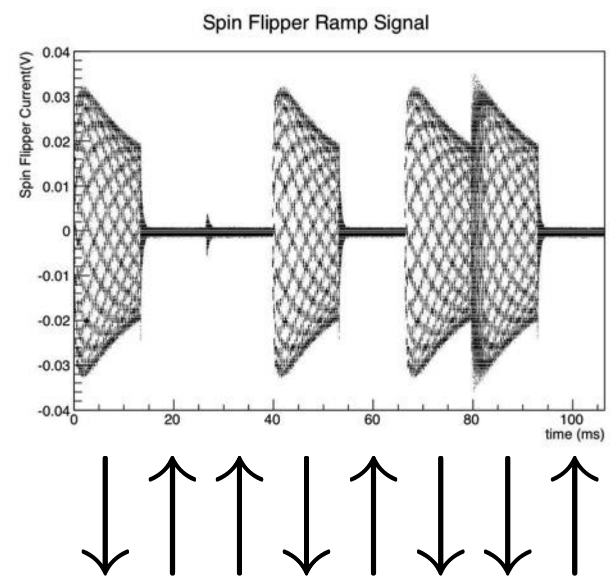

16L liquid para-hydrogen target

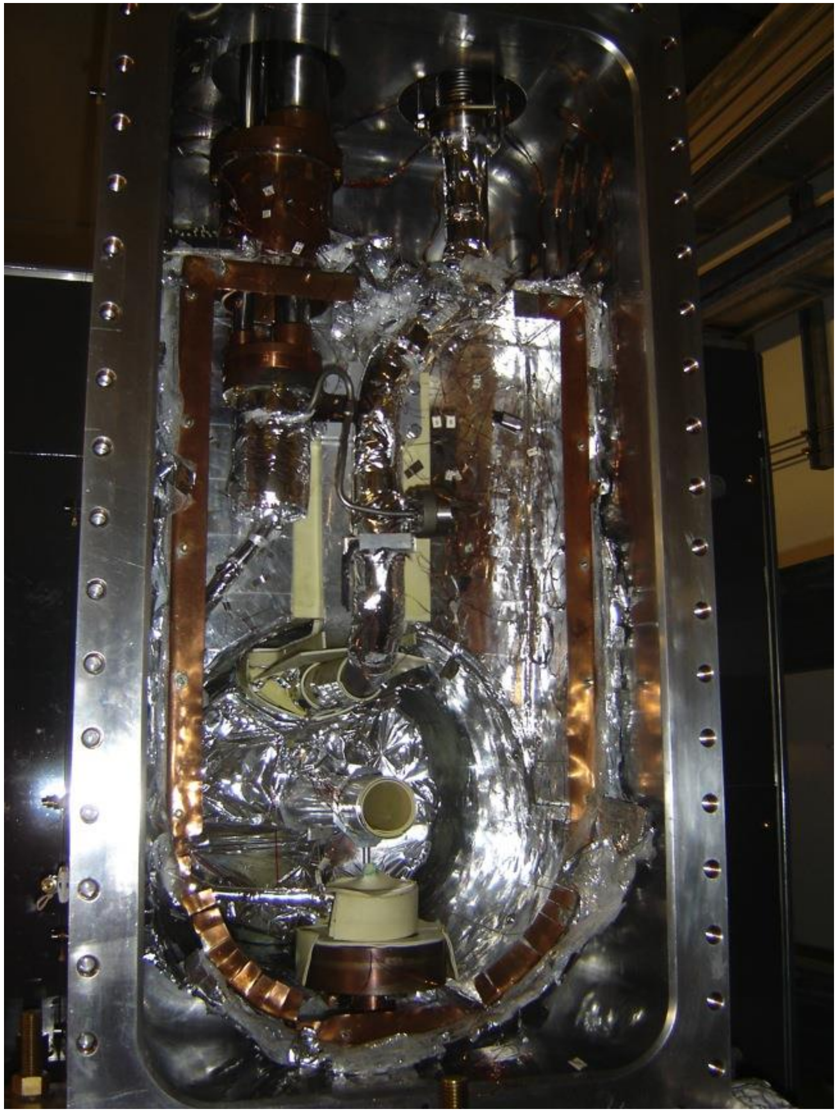

- 30 cm long → 1 interaction length
- 99.97% para → 1% depolarization
- Improvements: pressure-stamped vessel
  thinner windows

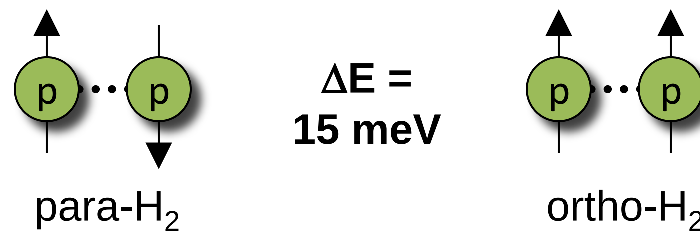

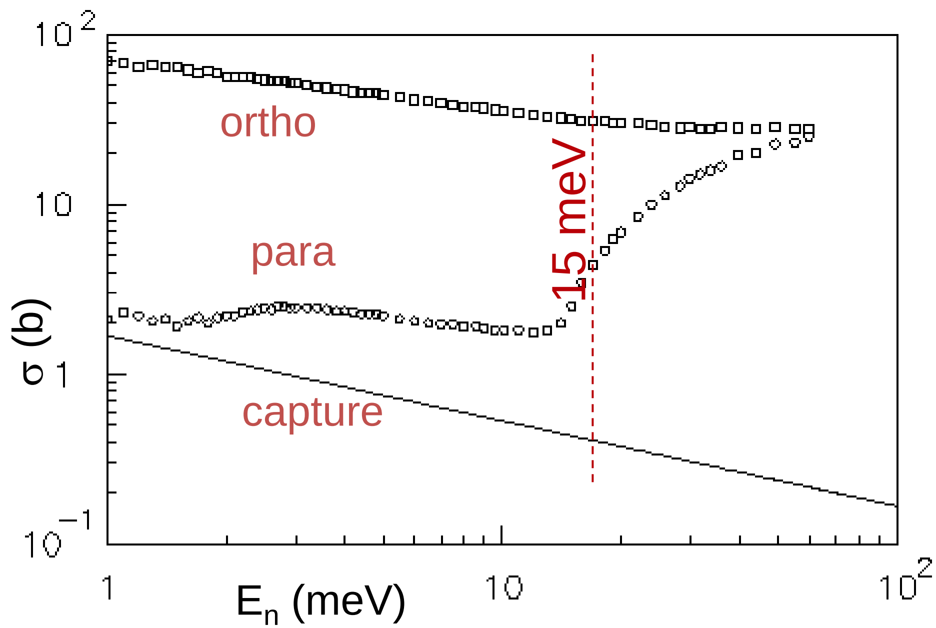

Ortho vs. Para H_2 neutron scattering

MCNP calculation of neutron beam intensity in liquid hydrogen target

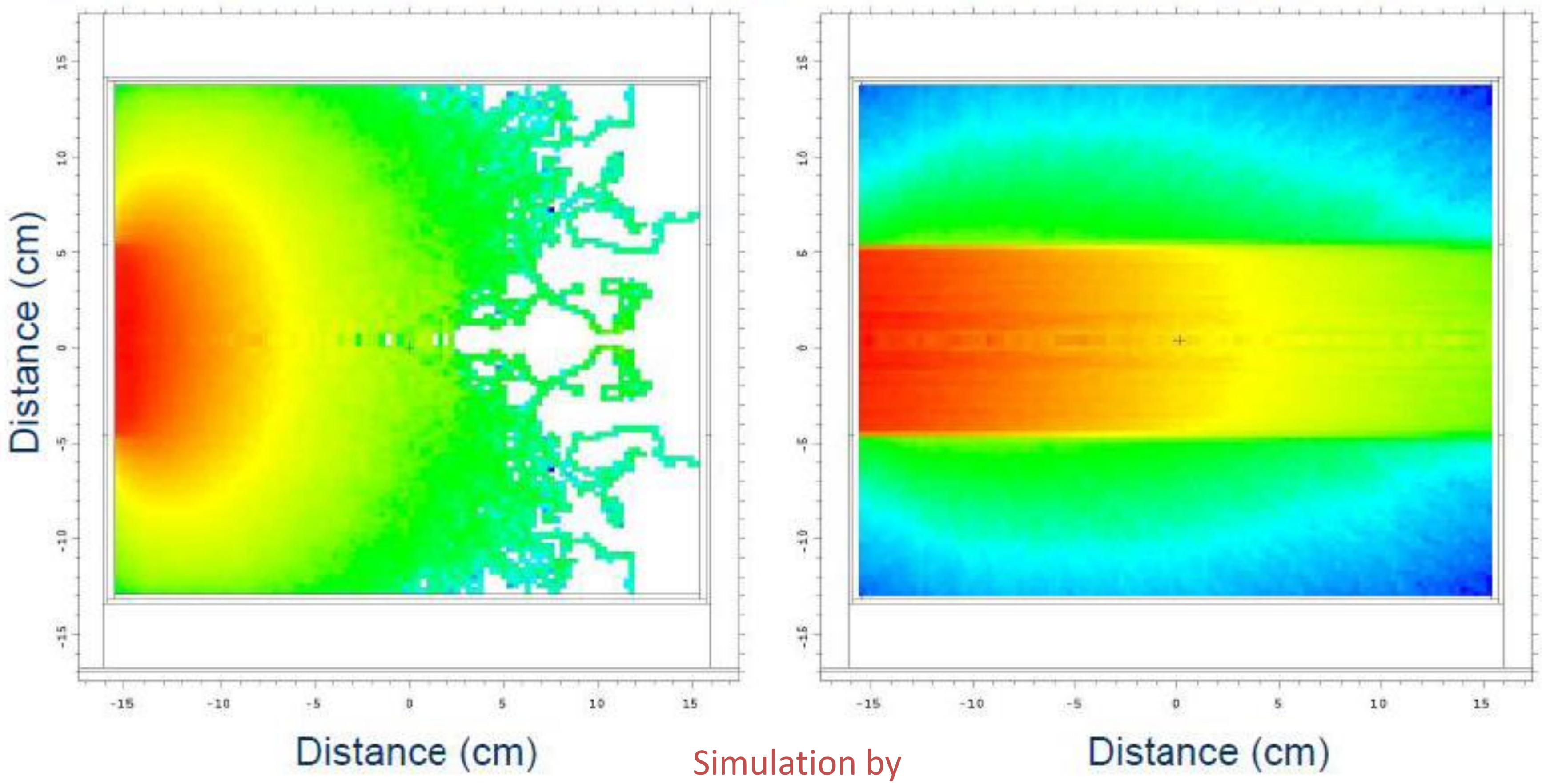

Pure Ortho - H_2

Simulation by
Kyle Grammer

Pure Para - H_2

L. Barron-Palos *et al.,* Nucl. Instr. Meth. **A671** 137 (2012)

CsI(Tl) Detector Array

- 4 rings of 12 detectors each
  - 15 x 15 x 15 cm^3 each
- VPD's insensitive to B field
- detection efficiency: 95%
- current-mode operation
  - 5 x 10^7 gammas/pulse
  - counting statistics limited

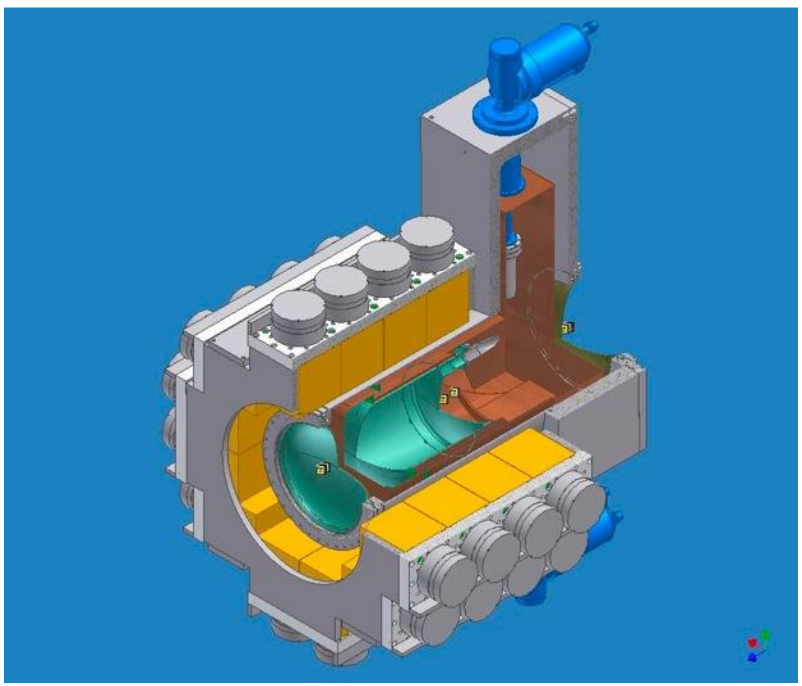

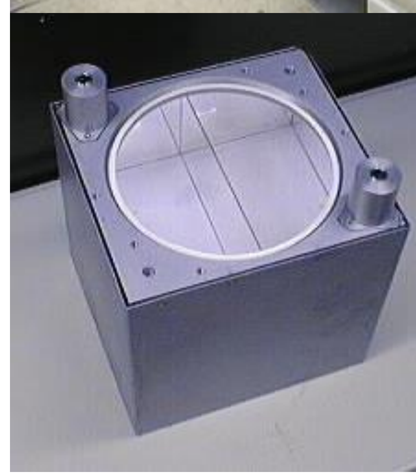

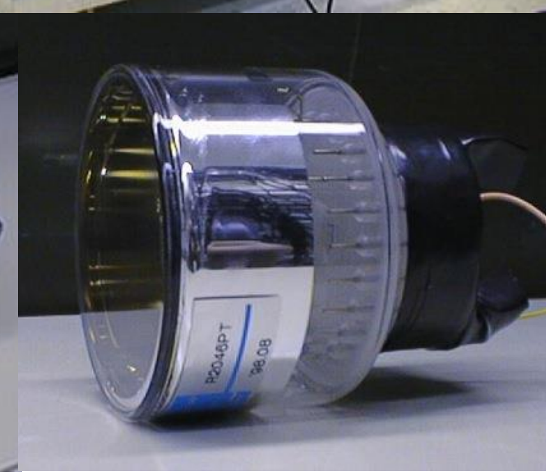

Background Sub. & Geometry Factors

$$A_\gamma^{np} = \frac{A_{raw}}{P_n \epsilon_{sf} C_d} - F_{BG} \frac{A_{Al}}{P_n^{Al} \epsilon_{sf}^{Al} C_d^{Al}}$$

Aluminum asymmetry

neutron pol.

RFSF eff.

target depol.

Aluminum background

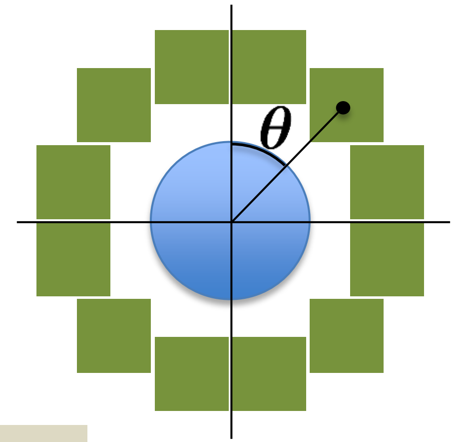

UP-DOWN

LEFT-RIGHT

$$A_{raw} = A_\gamma^{PV} G_{UD} + A_\gamma^{PC} G_{LR} + A_{offset}$$

$$\langle s_n \cdot k_\gamma = \cos\theta \rangle$$

$$\langle s_n \cdot k_n \times k_\gamma = \sin\theta \rangle$$

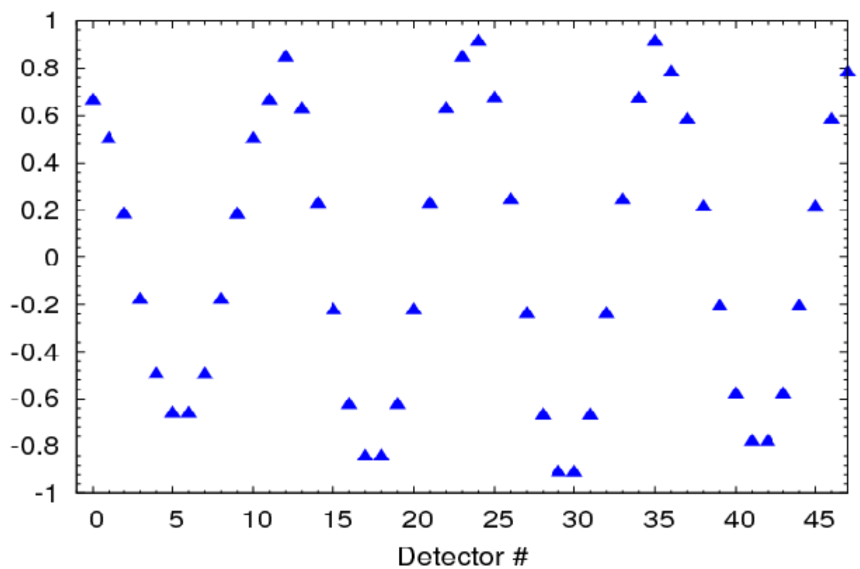

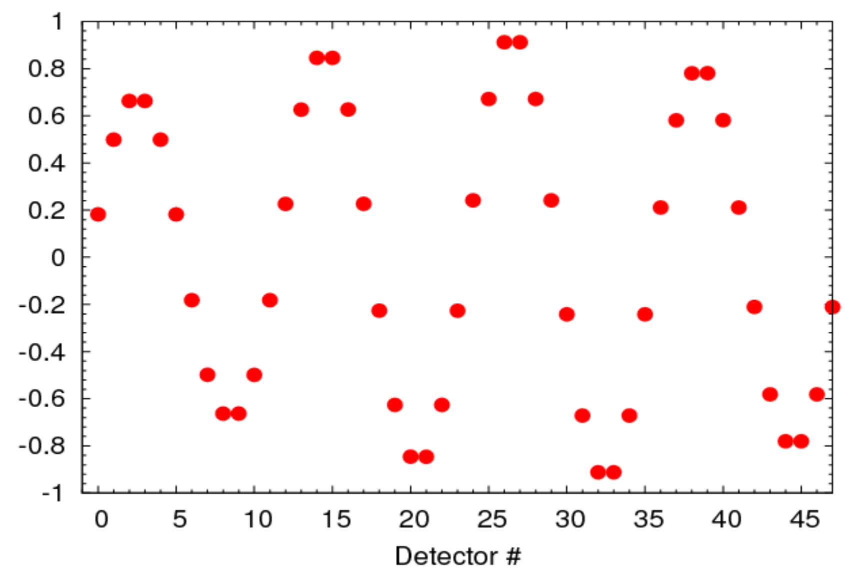

Chlorine PV asymmetry

- Data set
  - 40 hr. over 4 run periods
- Corrections
  - Background Subtraction
  - Beam Polarization
  - Beam Depolarization
  - RFSF Efficiency
  - Geometric factors (1% uncertainty)

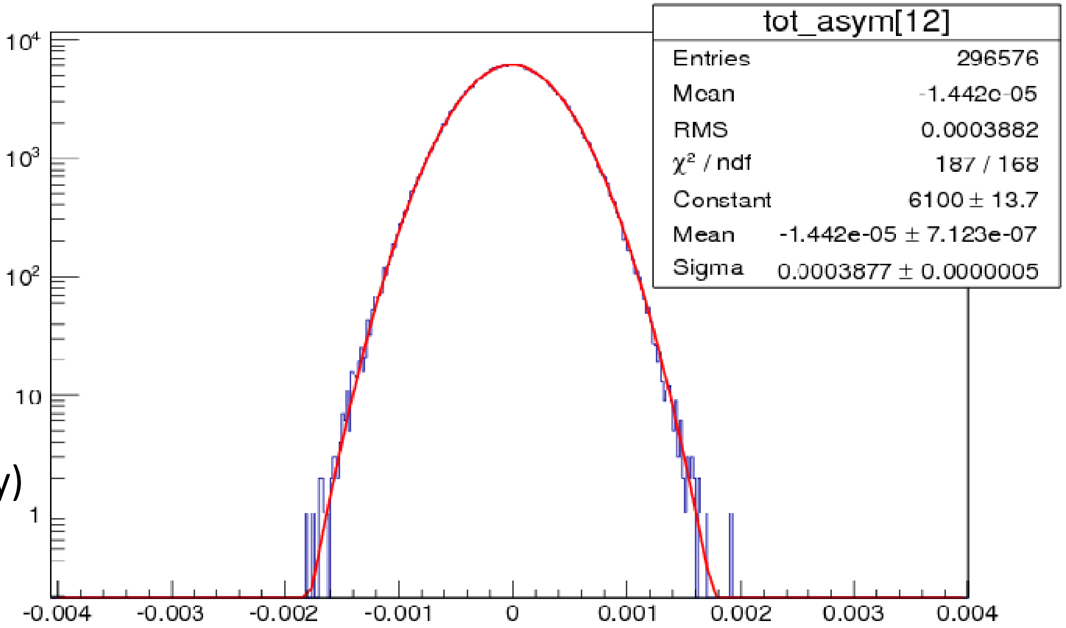

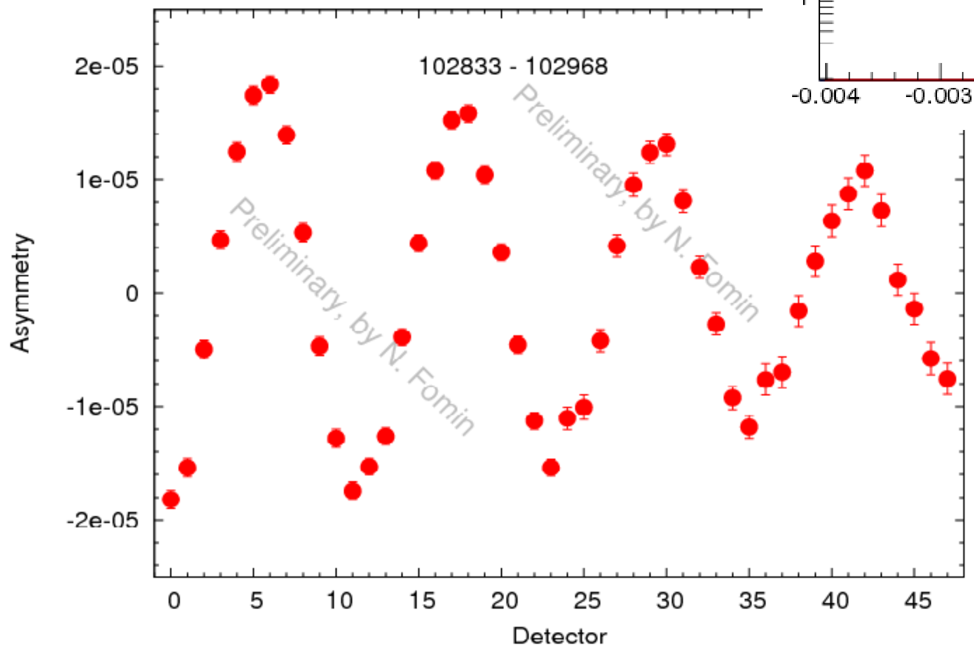

Measurement	Asymmetry (x10^{-6})
LANL	-29.1 ± 6.7
Leningrad	-27.8 ± 4.9
ILL	-21.2 ± 1.72
SNS (Current result)	-25.9 ± 0.6

Aluminum Asymmetry

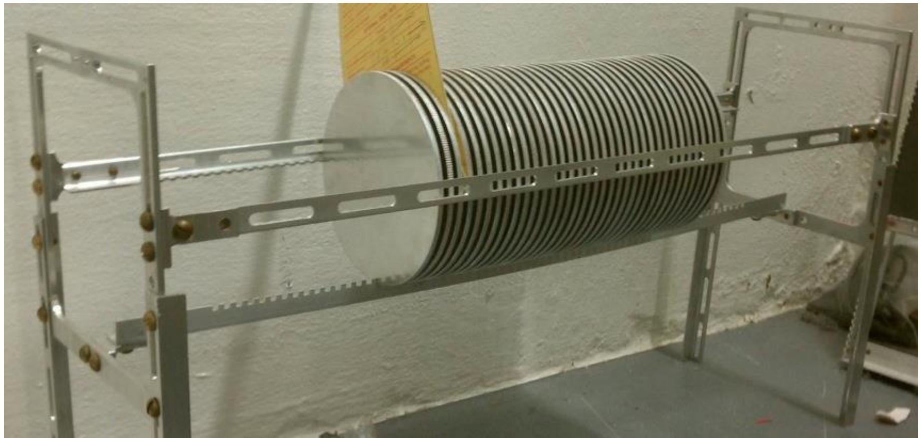

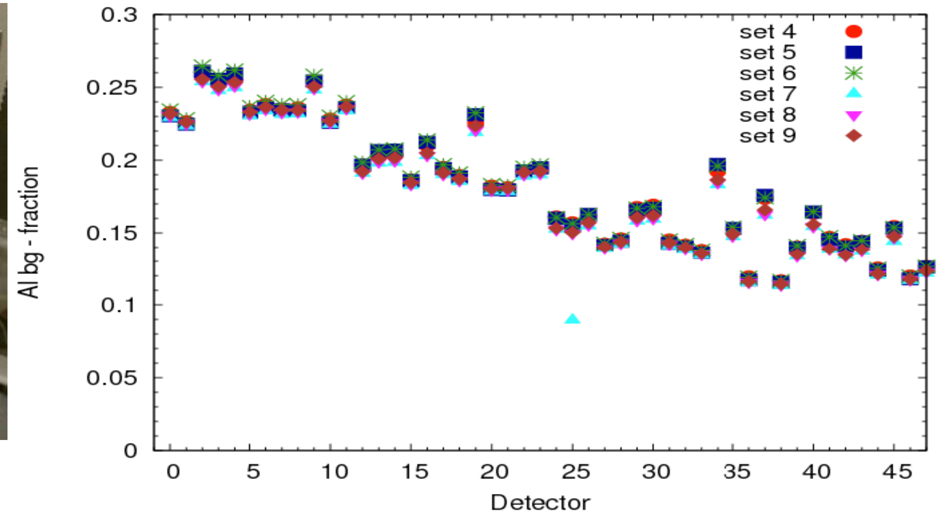

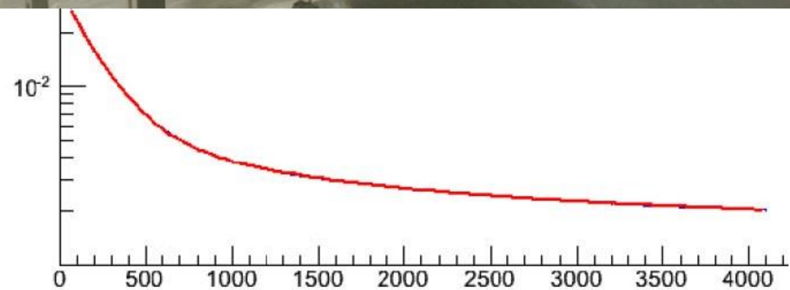

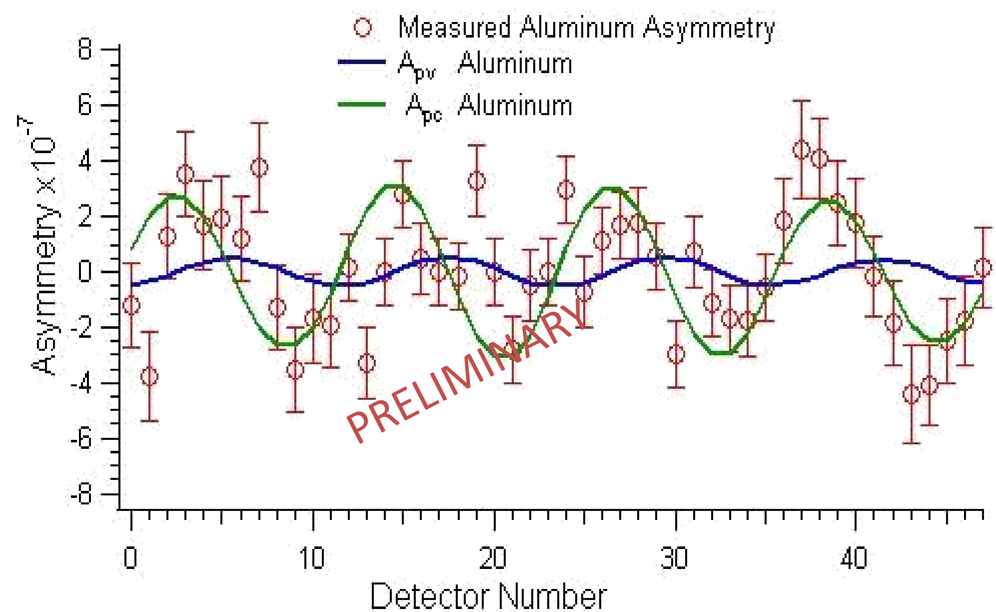

- Dominant systematic effect
  - 15–25% background at SNS
- Extracted from decay amplitude
  - Lifetime τ = 27 min
- Must measure δA = 3 x 10^{-8}

Recent Hydrogen Data

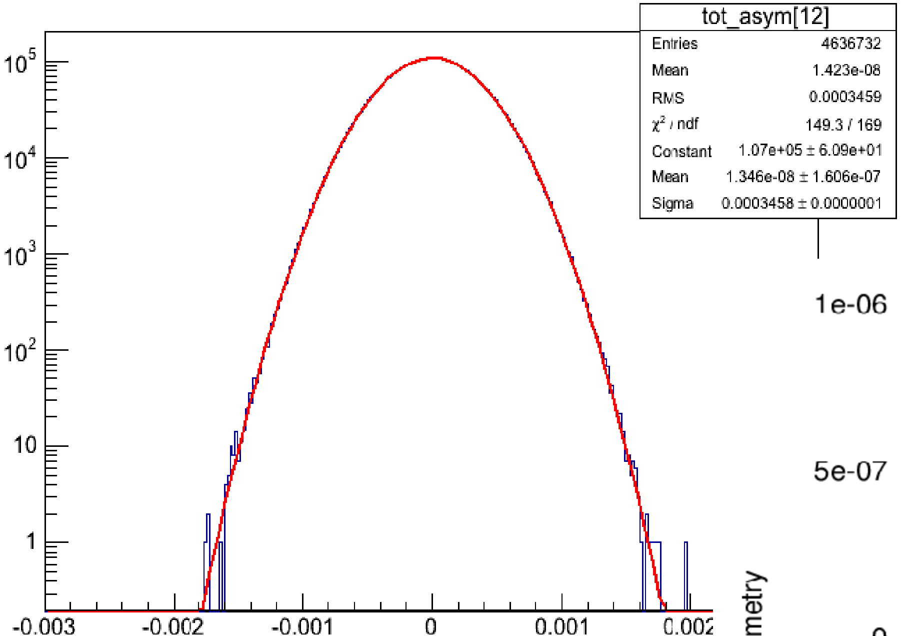

- Shown: 200 hr. data from Fall 2012
- Completed full data set June 2014

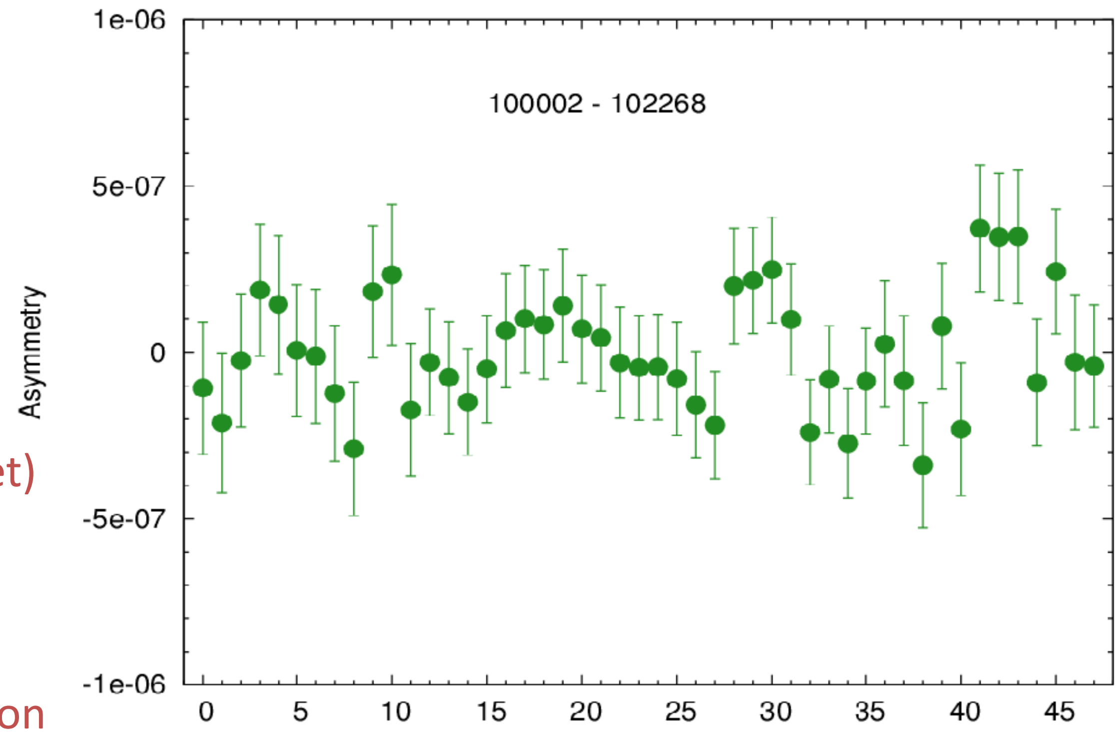

- Preliminary result (~10% dataset)
  A_{UD} = (-7.14 ± 4.4) x 10^{-8}
  A_{LR} = (-0.91 ± 4.3) x 10^{-8}

- Full results to be announced soon
  δA approximately **13 ppb**

Systematic & Statistical Uncertainties

Systematic Effects which may cause false Asym	Size
Additive Asymmetry (instrumental)	$< 1\times10^{-9}$
Multiplicative Asymmetry (instrumental)	$< 1\times10^{-9}$
Stern-Gerlach (steering of the beam)	$< 1\times10^{-10}$
γ – ray circular polarization	$< 1\times10^{-12}$
β – decay in flight	$< 1\times10^{-11}$
Capture on ^{6}Li	$< 1\times10^{-11}$
Radiative β –decay	$< 1\times10^{-12}$
β - delayed Al gammas (internal + external)	$< 1\times10^{-9}$
Uncertainties in applied corrections	
Neutron beam polarization uncertainty	< 2%
RFSF efficiency uncertainty	~ 0.5%
Depolarization of the neutron beam	< 0.5% (target-dependent)
Uncertainty in geometric factors	1%
Polarization of overlap neutrons	0.1%
Target Position	0.03%
Statistical uncertainty in presented results	
Combined hydrogen and aluminum data	$\sim 4.5\times10^{-8}$

n-^{3}He Collaboration

R. Alarcon[1], S. Baeßler[3], S. Balascuta[1], L. Barron-Palos[2], A. Barzilov[7], D. Bowman[4], J. Calarco[9], V. Cianciolo[4], C. Crawford[5], J. Favela[2], N. Fomin[4,13], I. Garishvili[13], M. Gericke[6], C. Gillis[8], G. Greene[4,13], V. Gudkov[11], J. Hamblen[12], C. Hayes[13], E. Iverson[4], K. Latiful[5], S. Kucuker[13], M. Maldonado-Velazquez[2], M. McCrea[6], I. Novikov[15], C. Olguin[6], S. Penttila[4], E. Plemons[12], A. Ramirez[2], P.-N. Seo[14], Y. Song[11], A. Sprow[5], J. Thomison[4], T. Tong[4], M. Viviani[10], C. Wichersham[12]

[1]Arizona State University
[2]Universidad Nacional Autonoma de Mexico
[3]University of Virginia
[4]Oak Ridge National Laboratory
[5]University of Kentucky
[6]University of Manitoba, Canada
[7]Univeristy of Nevada at Los Vegas
[8]Indiana University
[9]University of New Hampshire
[10]Instituto Nazionale di Fisica Nucleare, Sezione di Pisa
[11]University of South Carolina
[12]University of Tennessee at Chattanooga
[13]University of Tennessee, Knoxville
[14]Duke University
[15]Western Kentucky University

n-^{3}He Reaction

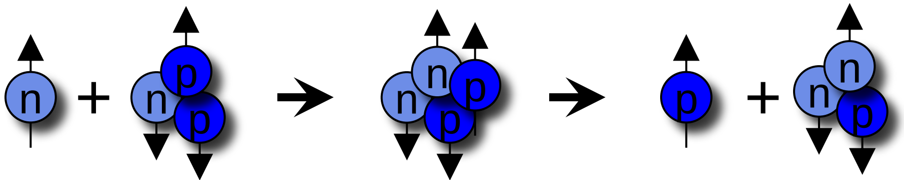

$$\vec{n} + {}^3\mathrm{He} \rightarrow \mathrm{p} + \mathrm{t} + 764\ \mathrm{keV}$$

S(I): $\frac{1}{2}\left(\frac{1}{2}\right) + \frac{1}{2}\left(\frac{1}{2}\right) \rightarrow \frac{1}{2}\left(\frac{1}{2}\right) + \frac{1}{2}\left(\frac{1}{2}\right)$

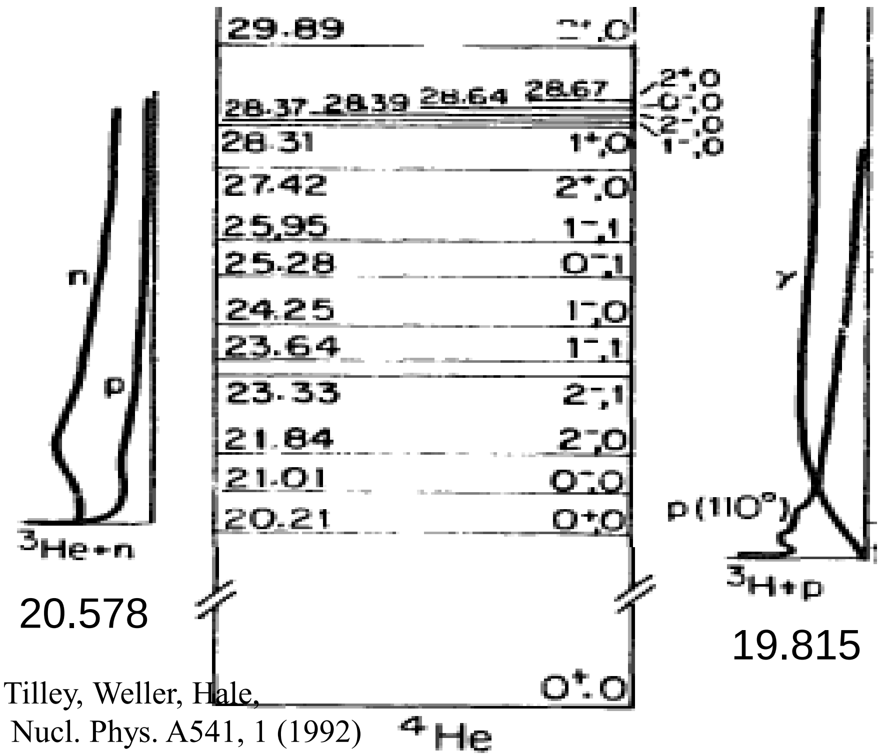

Tilley, Weller, Hale,
Nucl. Phys. A541, 1 (1992)

PV observables:

$\sigma_n \cdot k_n$ ~ k_n very small for low-energy neutrons

$\sigma_n \cdot k_p$, $\sigma_n \cdot k_t$
- essentially the same asym.
- must discriminate between back-to-back proton-triton

- 4He $J^\pi = 0^+$ resonance $^1S_0(I=0) \leftrightarrow {}^3P_0(I=0)$
- sensitive to EFT coupling $\lambda_s^{I=0}$ or DDH couplings $h_\rho^0,\ h_\omega^0$
- ~10% ΔI=1 contribution (Gerry Hale, qualitative)
- A ~ -1–3x10^{-7} (M. Viviani, PISA)
- A ~ -1–4x10^{-7} (Gudkov) mixing between 0^+, 0^- resonance
- Naïve scaling of p-p scattering at 22.5 MeV: A ~ 5x10^{-8}

Experimental setup

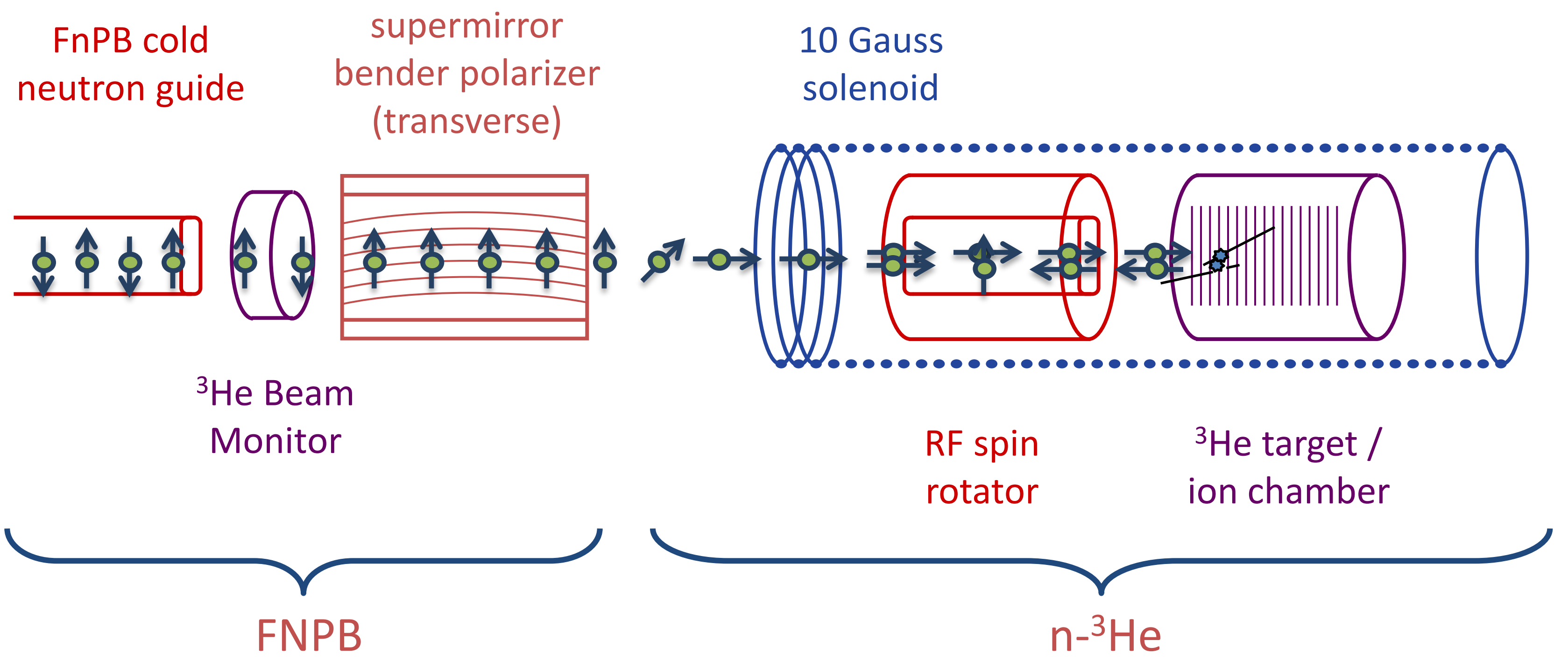

- longitudinal holding field – suppressed PC nuclear asymmetry
  A=1.7x10^{-6} (Hales) $s_n \bullet k_n \times k_p$ suppressed by two small angles
- RF spin flipper – negligible spin-dependence of neutron velocity
- ^{3}He ion chamber – both target and detector

Solenoid

- Definition of σ_n direction
  - Adiabatic rotation from transverse to longitudinal spin
  - 10 mG, 0.1% uniformity

Univ. Nacional Autónoma de México



3-axis fluxgate calibration

- Same principle as normalizing a level
- Fit for three voltage offsets + full 3x3 response matrix

$$\vec{m}^{\alpha\beta} = R S^{\alpha} \vec{b}^{\beta} + \vec{m}_0 \qquad \vec{m}^{\alpha\beta} = \text{meas},\ S^{\alpha} = \text{sym},\ R = \text{resp},\ \vec{b}^{\beta} = \text{field}$$

$$m_i^{\alpha} = R_{ij} S^{\alpha}_{jk} b_k + m_{0i}$$

$$\begin{pmatrix} m_1^1 & m_2^1 & m_3^1 \\ m_1^2 & m_2^2 & m_3^2 \\ \vdots & & \\ m_{16}^1 & m_{16}^2 & m_{16}^3 \end{pmatrix}_{16\,(\alpha)\times 3\,(i)} = \begin{pmatrix} S^1_{11} & S^1_{12} & S^1_{13} & S^1_{21} & S^1_{22} & S^1_{23} & S^1_{31} & S^1_{32} & S^1_{33} & 1 \\ S_{11} & S_{12} & S_{13} & S_{21} & S_{22} & S_{23} & S_{31} & S_{32} & S_{33} & 1 \\ \vdots & & \vdots & & & \vdots & & & \vdots & \\ S^{16}_{11} & S^{16}_{12} & S^{16}_{13} & S^{16}_{21} & S^{16}_{22} & S^{16}_{23} & S^{16}_{31} & S^{16}_{32} & S^{16}_{33} & 1 \end{pmatrix}_{16\,(\alpha)\times 10\,(jk+1)} \begin{pmatrix} \begin{pmatrix} R_{11} & R_{21} & R_{31} \\ R_{12} & R_{22} & R_{32} \\ R_{13} & R_{23} & R_{33} \end{pmatrix} \otimes \begin{pmatrix} b_1 \\ b_2 \\ b_3 \end{pmatrix} \\ \hline m_0^1 \quad m_0^2 \quad m_0^3 \end{pmatrix}_{3\,(i)}$$

$$\text{or} \quad M = (S \mid 1)\left(\frac{R^T \otimes b}{m}\right).$$

3-axis fluxgate calibration

$$ {}_9T_3 = {}_3R_3 \otimes {}_3b_1 = \begin{pmatrix} R_{11} & R_{21} & R_{31} \\ R_{12} & R_{22} & R_{32} \\ R_{13} & R_{23} & R_{33} \end{pmatrix} \otimes \begin{pmatrix} b_1 \\ b_2 \\ b_3 \end{pmatrix} = \begin{pmatrix} R_{11}b_1 & R_{21}b_1 & R_{31}b_1 \\ R_{11}b_2 & R_{21}b_2 & R_{31}b_2 \\ R_{11}b_3 & R_{21}b_3 & R_{31}b_3 \\ \hdashline R_{12}b_1 & R_{22}b_1 & R_{32}b_1 \\ R_{12}b_2 & R_{22}b_2 & R_{32}b_2 \\ R_{12}b_3 & R_{22}b_3 & R_{32}b_3 \\ \hdashline R_{13}b_1 & R_{23}b_1 & R_{33}b_1 \\ R_{13}b_2 & R_{23}b_2 & R_{33}b_2 \\ R_{13}b_3 & R_{23}b_3 & R_{33}b_3 \end{pmatrix} $$

Rearrange this matrix into $\mathcal{T} = \mathcal{R}\, b$

$$ \begin{pmatrix} T_{11} & T_{21} & T_{31} \\ T_{12} & T_{22} & T_{32} \\ T_{13} & T_{23} & T_{33} \\ \hdashline T_{41} & T_{51} & T_{61} \\ T_{42} & T_{52} & T_{62} \\ T_{43} & T_{53} & T_{63} \\ \hdashline T_{71} & T_{81} & T_{91} \\ T_{72} & T_{82} & T_{92} \\ T_{73} & T_{83} & T_{93} \end{pmatrix} = \begin{pmatrix} R_{11} \\ R_{21} \\ R_{31} \\ \hdashline R_{12} \\ R_{22} \\ R_{32} \\ \hdashline R_{13} \\ R_{23} \\ R_{33} \end{pmatrix} \begin{pmatrix} b_1 & b_2 & b_3 \end{pmatrix} $$

or $\mathcal{T} = \mathcal{R}\, b$ and again

let $\mathcal{T} = U' \Delta V'^{T}$ (SVD) $= \hat{\mathcal{R}} \lambda_1 \hat{b} + \ldots$

$\hat{\mathcal{R}} \frac{\lambda}{B} \cdot B\hat{b}$

Then $\hat{\mathcal{R}}$ is the column of U' corresponding to the largest eigenvalue in Δ and $\hat{b}$ is the corresponding column of V'.

Transverse RF Spin Rotator

- Double-cosine-theta coil
  - Fringeless transverse RF field
  - Longitudinal OR transverse
  - Designed using scalar potential

Univ. Kentucky / Univ. Tennessee

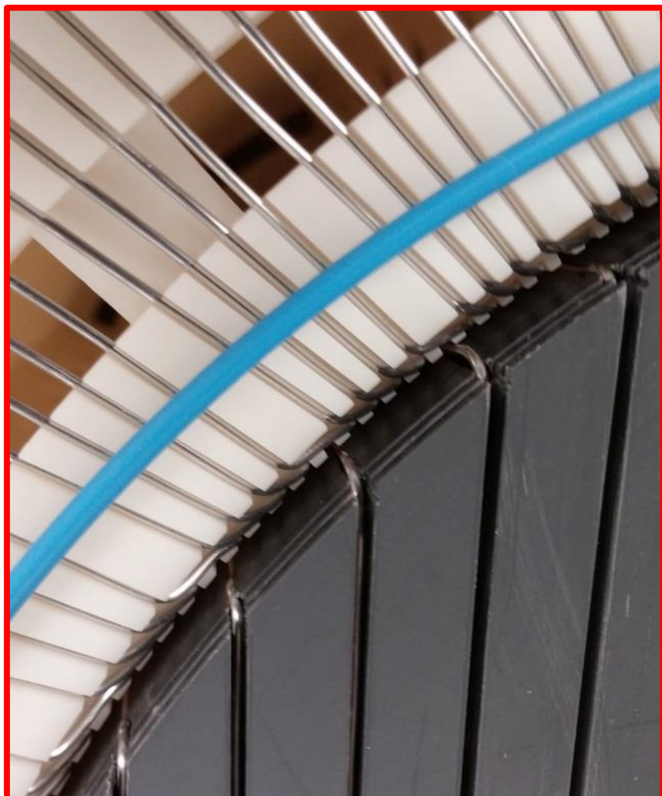

Magnetic Scalar Potential

	FLUX	FLOW
• **Field Equations**	$\Phi_B \equiv \int \boldsymbol{B}\cdot d\boldsymbol{a}$	$\mathcal{E}_H \equiv \int \boldsymbol{H}\cdot d\boldsymbol{l} = \Delta U$
field	$\nabla \cdot \boldsymbol{B} = 0$	$\nabla \times \boldsymbol{H} = \boldsymbol{J}$
potential	$-\nabla \cdot \mu \nabla U = 0$	$\boldsymbol{H} = -\nabla U \quad \{\boldsymbol{J} = \boldsymbol{0}\}$
• **Boundary conditions**		
field	$\hat{\boldsymbol{n}} \cdot \Delta \boldsymbol{B} = 0$	$\hat{\boldsymbol{n}} \times \Delta \boldsymbol{H} = \boldsymbol{K}$
potential	$\Delta(\mu \partial U / \partial n) = 0$	$U_2 - U_1 = \Delta I$

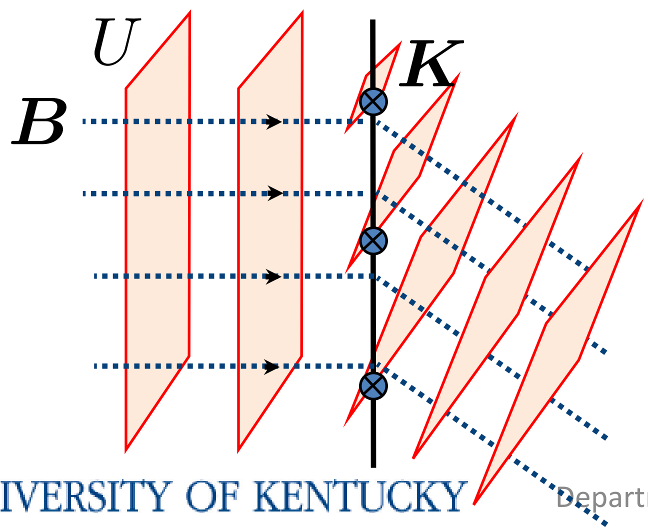

Magnetic flux lines $\quad \boldsymbol{B} = đ\Phi/d\boldsymbol{a}$

Magnetic flow sheets (scalar equipotential) $\quad U = \mathcal{E}(const)$

Surface Current $\quad \boldsymbol{K} = \Delta I/\Delta s$

Electric & Magnetic: Flux & Flow

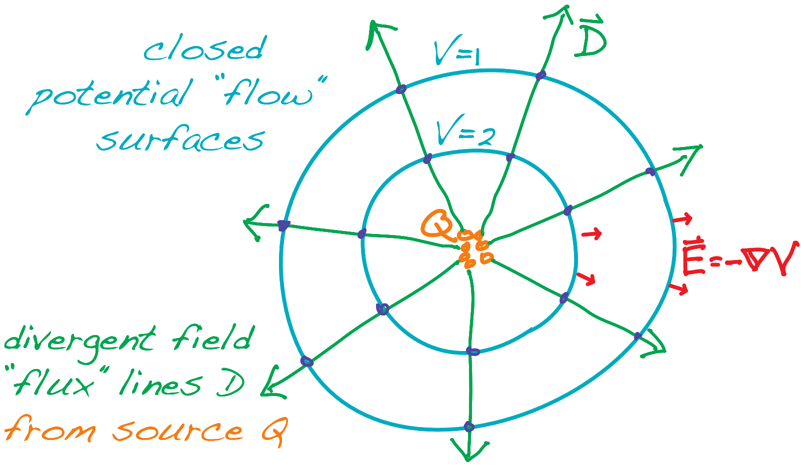

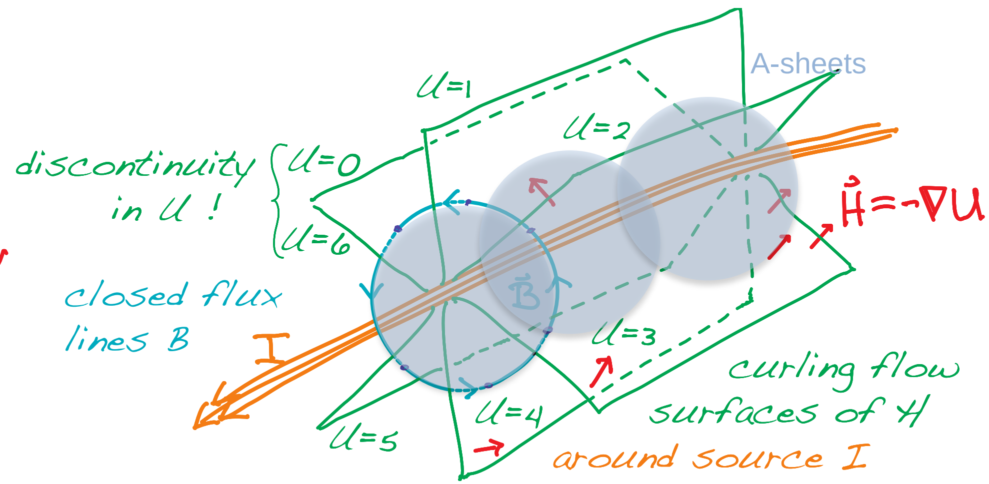

B.C.'s: Flux lines bounded by charge | Flux lines continuous

Flow sheets continuous (equipotentials) | Flow sheets bounded by current

Solenoid:

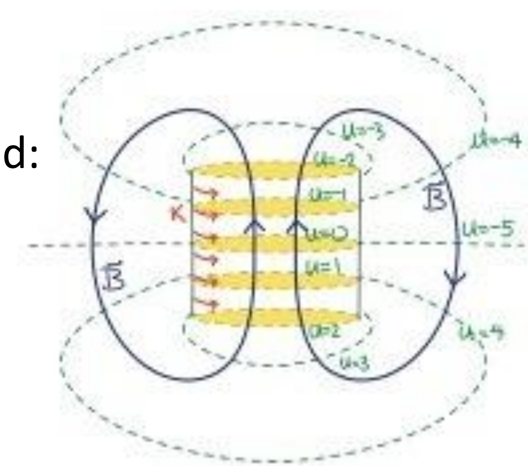

Cos-theta coil:

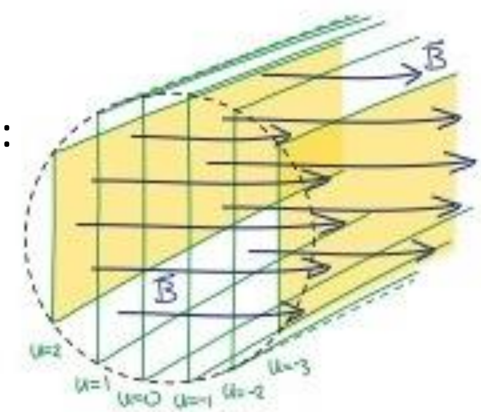

Calculation of optimal design

Based on physical interpretation of magnetic scalar potential U.

1. Solve Laplace equation for U imposing desired flux as boundary conditions

2. Wind the coil along equipotential contours along the boundary of each region (flow boundary cond.)

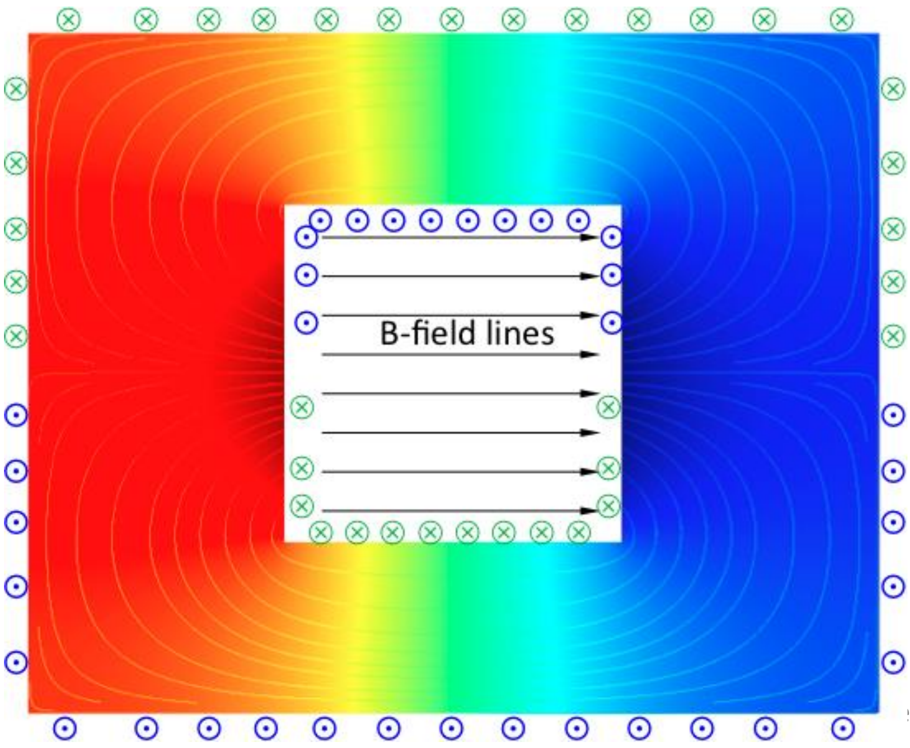

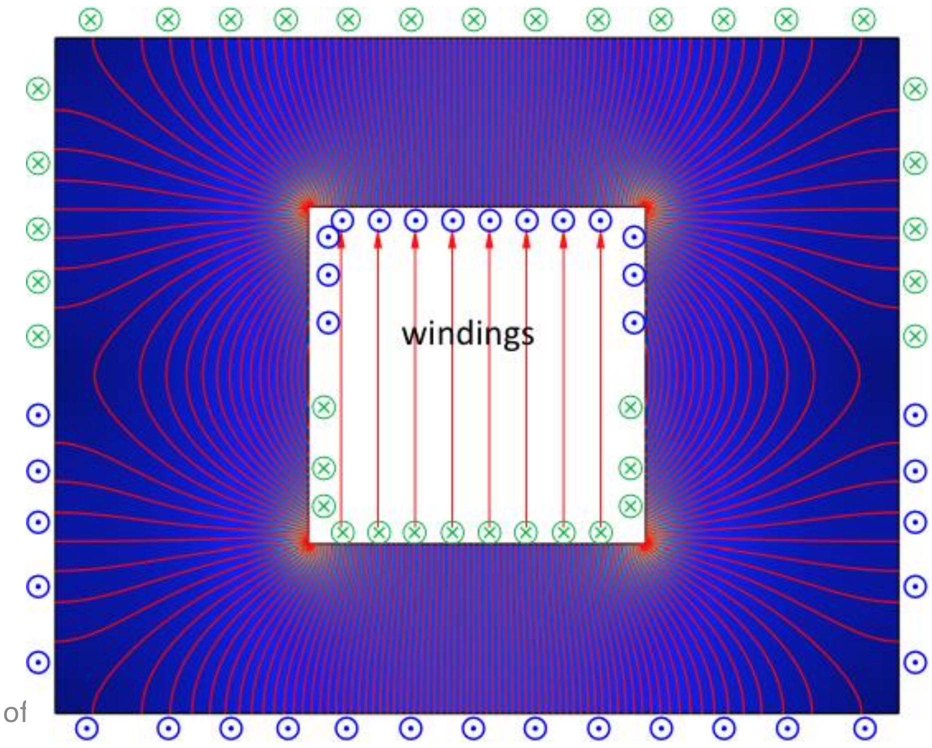

Transverse RFSR for n-^{3}He Exp.

- extension of NPDGamma design
  - TEM RF waveguide
- new resonator for n-^{3}He expt.
  - transverse horizontal RF B-field
  - longitudinal / transverse flipping
  - no fringe field - 100% efficiency
  - compact geometry – efficient
  - matched to driver electronics for NPDGamma spin flipper
- prototype design
  - parasitic with similar design for nEDM guide field near cryostat
  - fabrication, testing at UKy

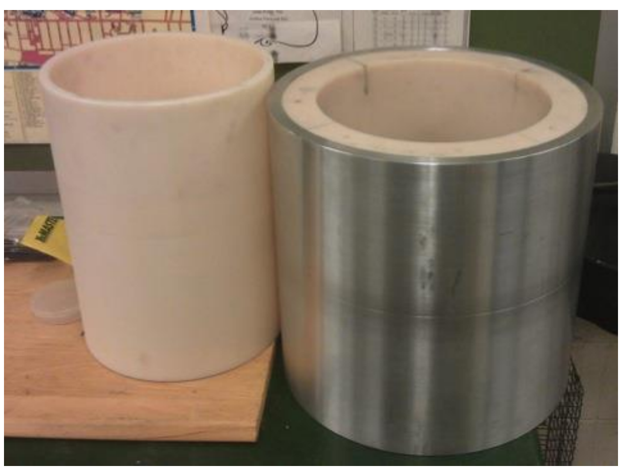

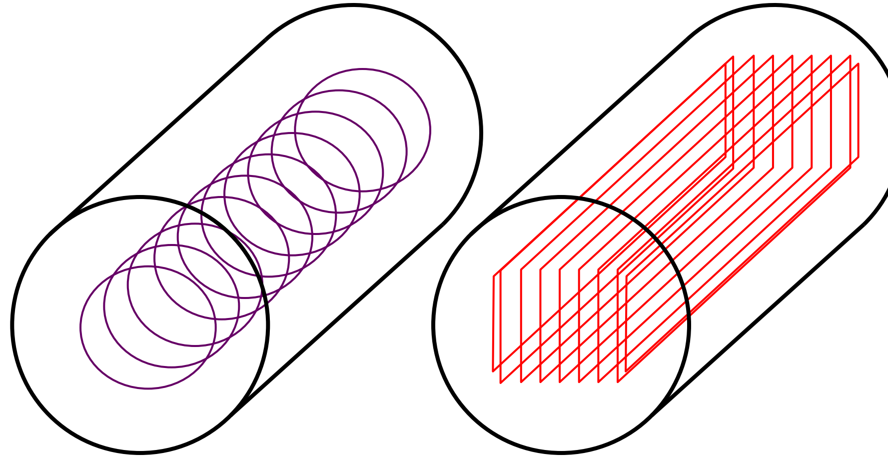

NPDGamma windings

n-^{3}He windings

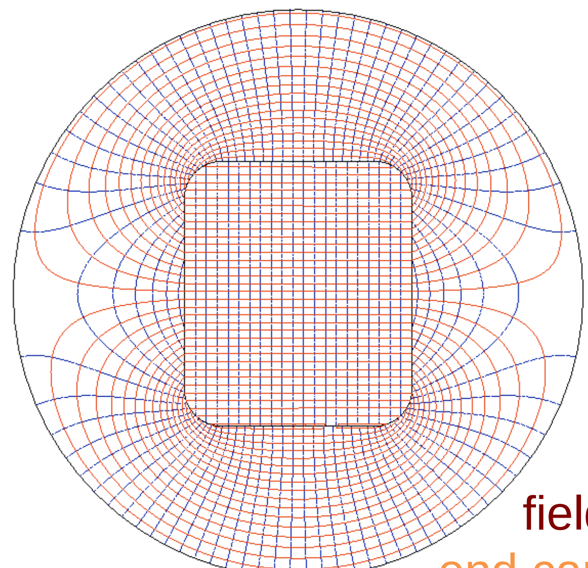

field lines

end cap windings

Prototype Double Cos-Theta Coil

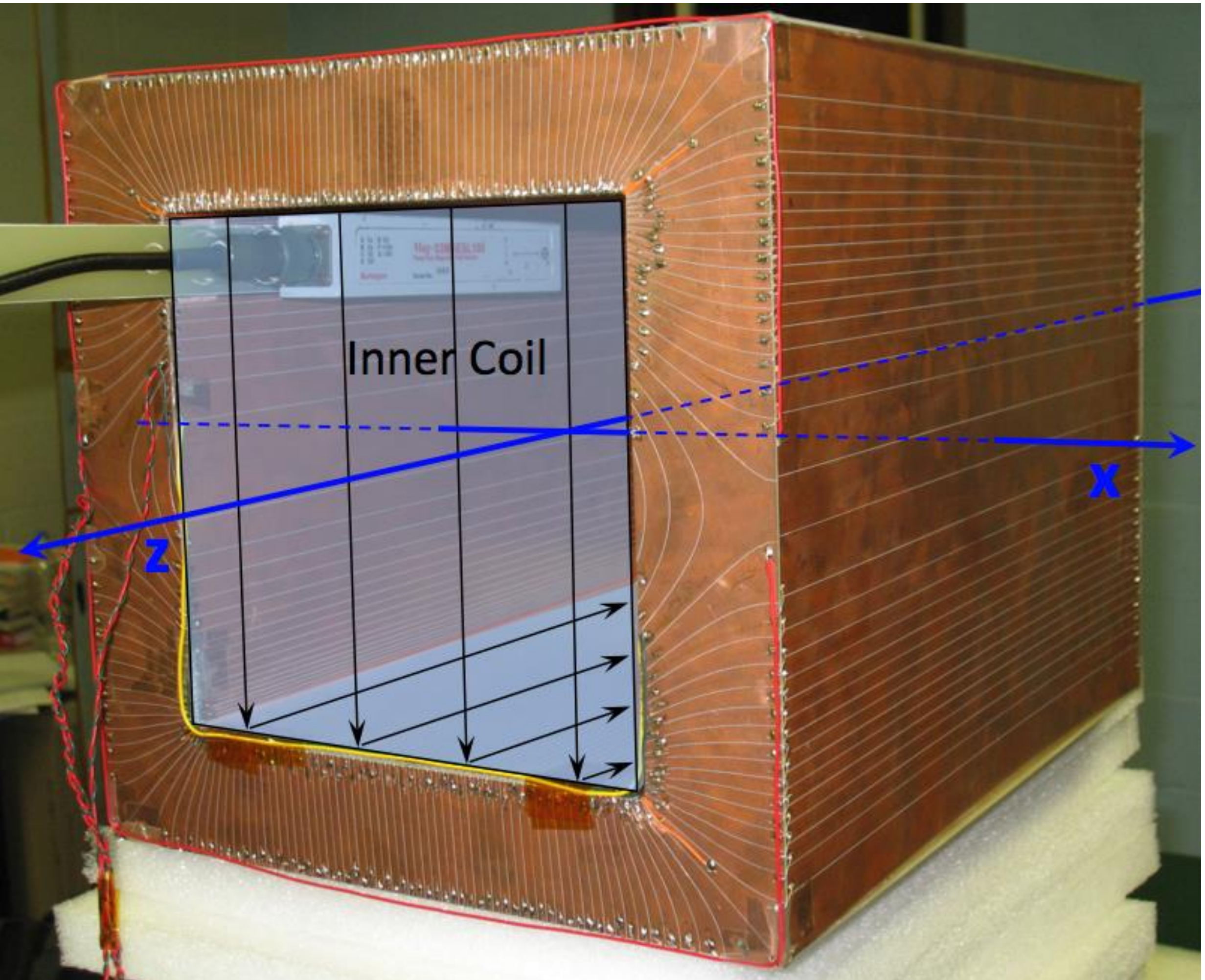

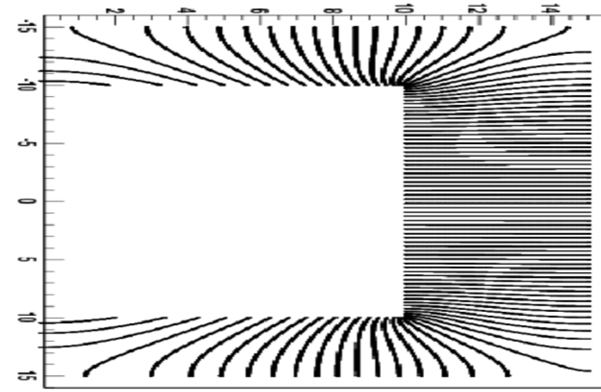

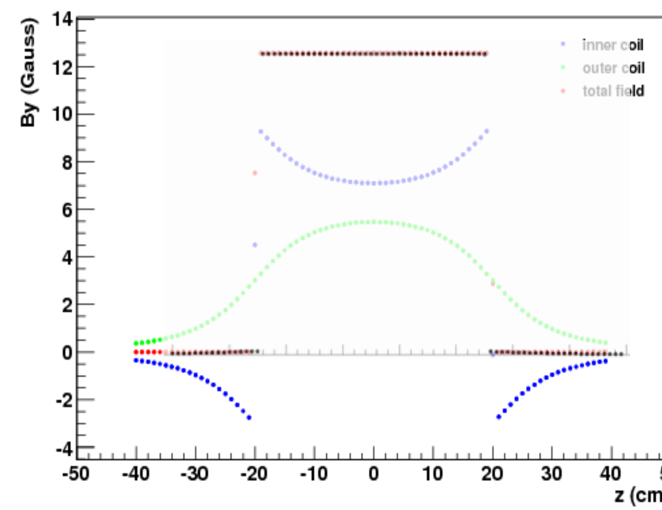

Collimator / Beam scanner

- Tune the beam size/axis for longitudinal/transverse asymmetry

U. Tennessee, UNAM, Arizona State U.

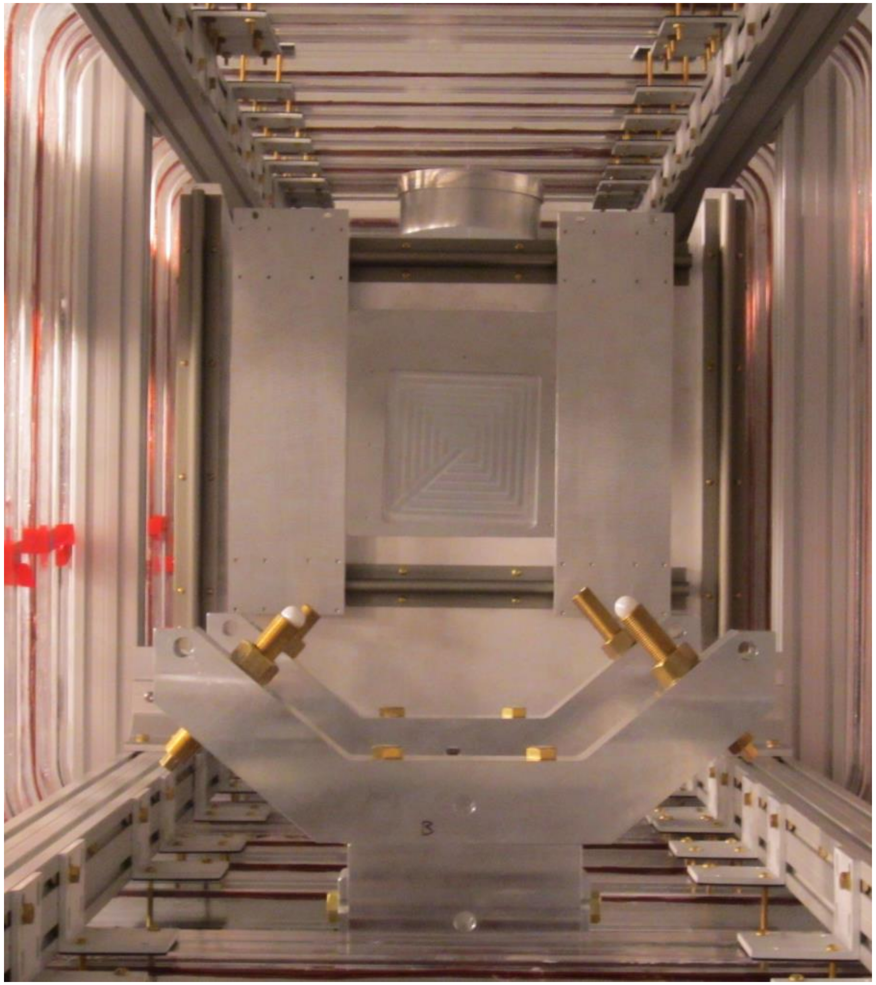

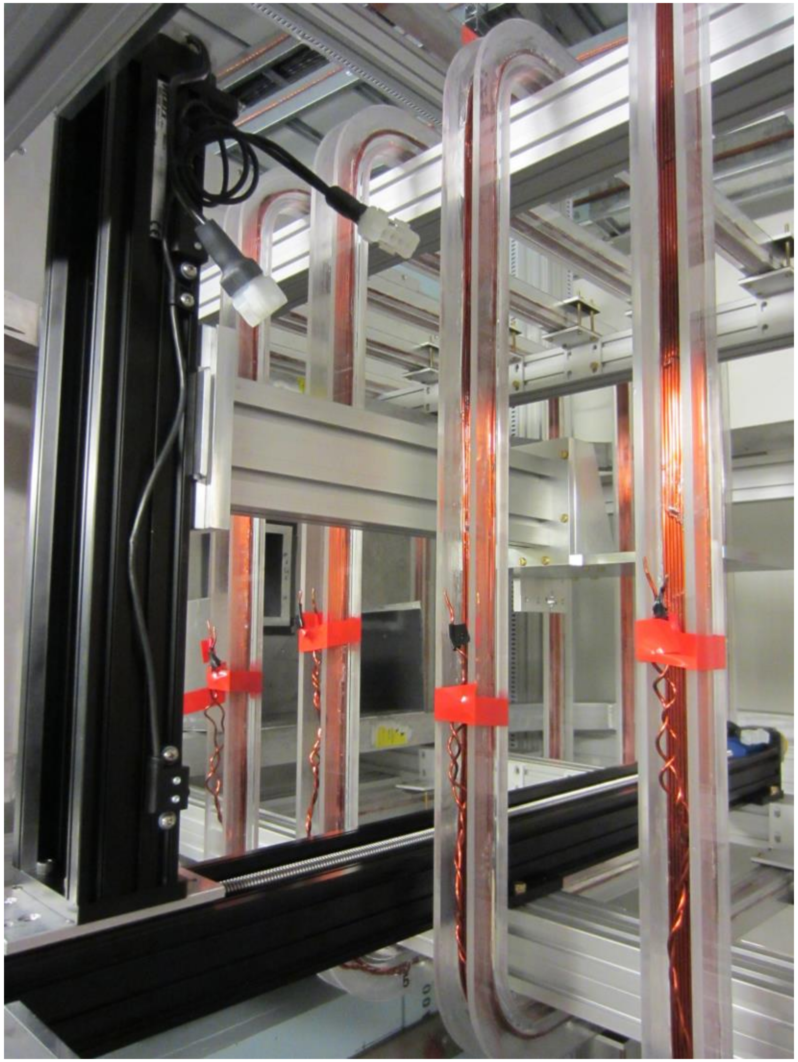

Active Target / Ion Chamber

- ^{3}He for both target and ionization gas
  - Macor frames with 9 x 16 sense wires, 8 x 17 HV wires
  - All aluminum chamber except for knife edges
  - 12” x 0.9 mm CF aluminum windows
  - 16 mCi tritium over life of experiment

University of Manitoba

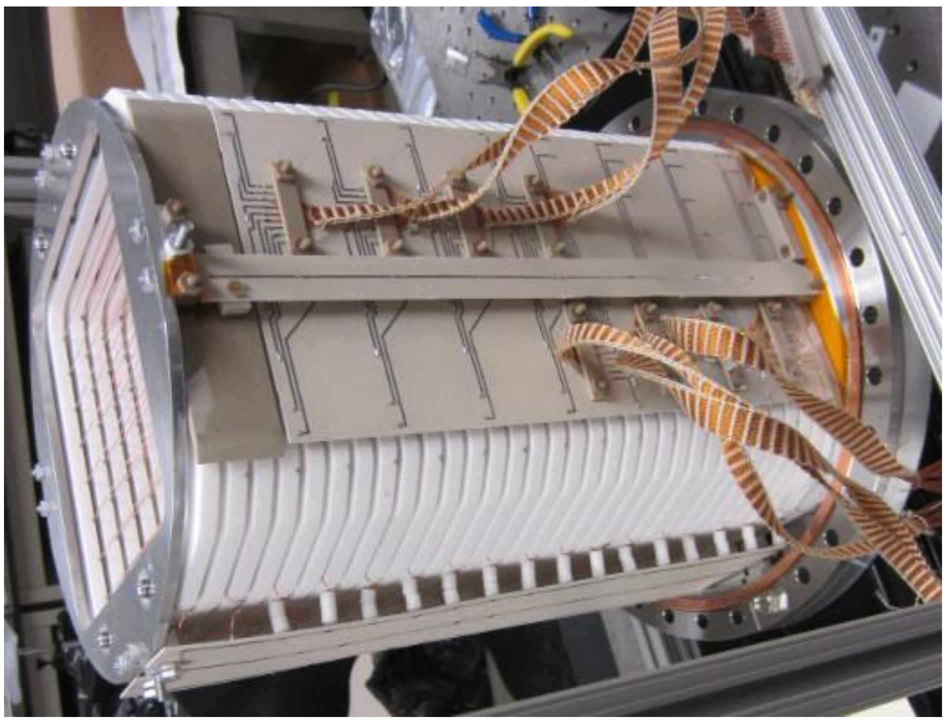

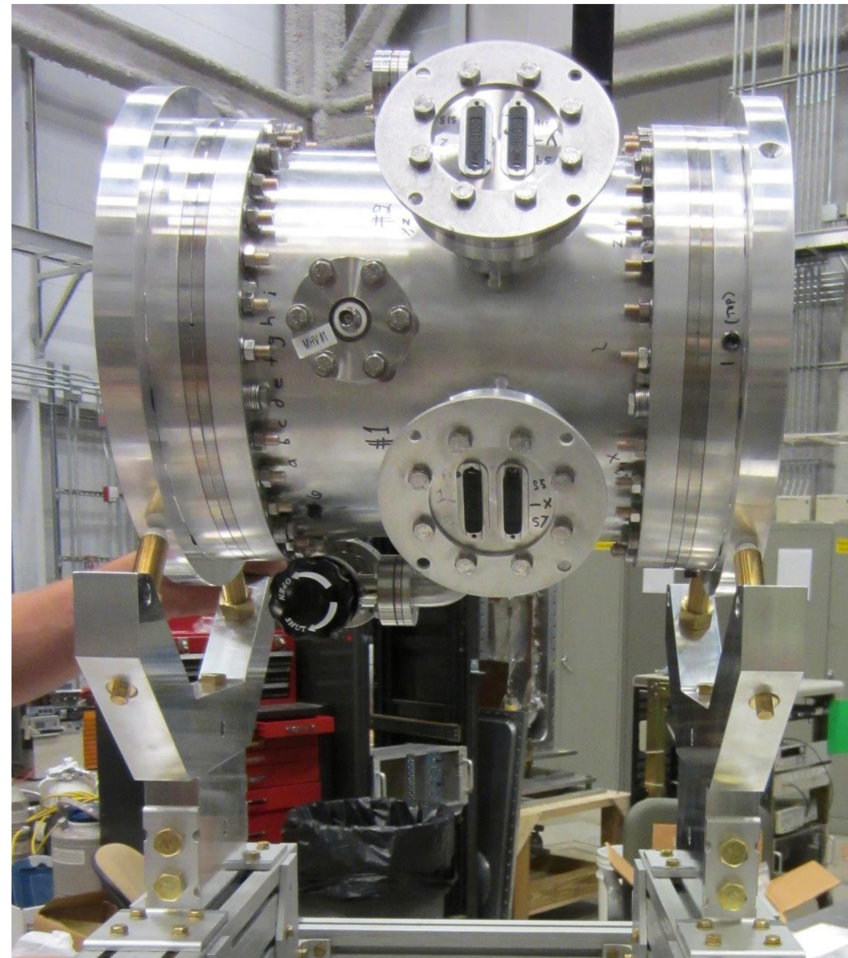

Readout Electronics

- Ionization read out in current mode
  - 144 channels read out simultaneously
  - Low-noise preamplifiers mount on chamber
  - 24-bit 100 kHz simultaneous sampling digitizers

Oak Ridge National Lab, Univ. Kentucky, Univ. Tennessee

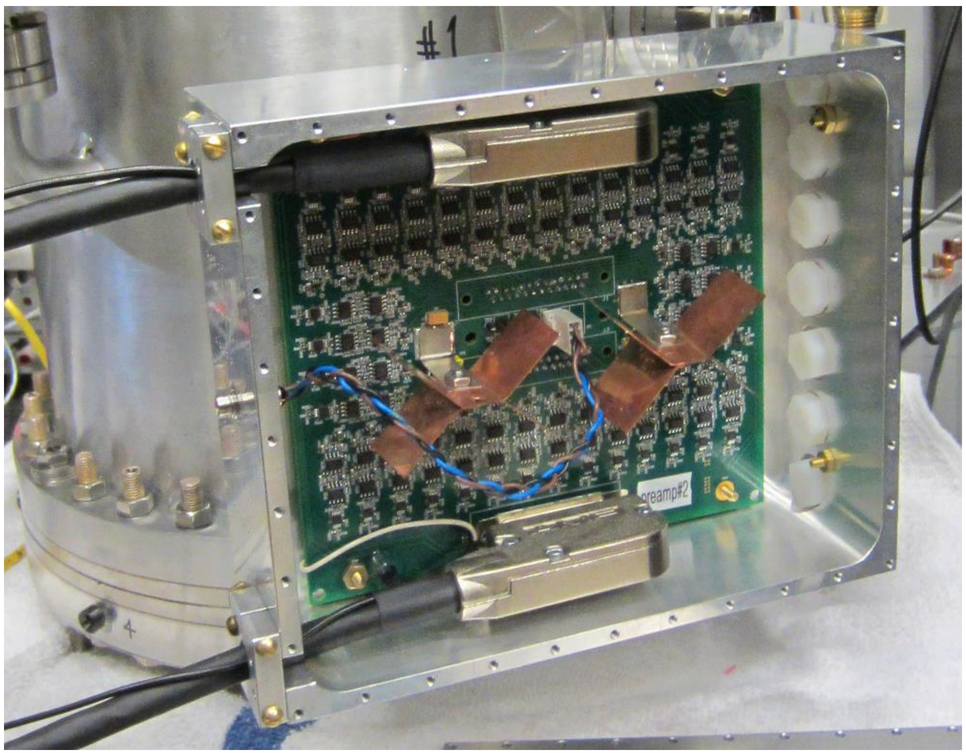

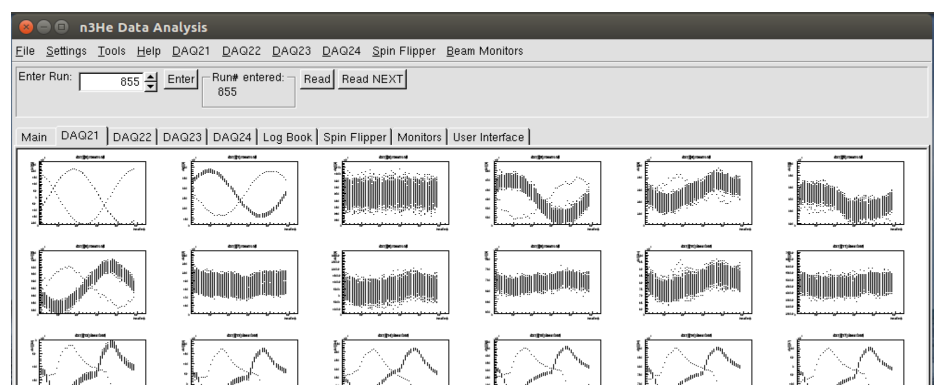

Commissioning data

- Instr. asymmetry, Beam scan, RFSF tune, Ion chamber tune
  - Completed Dec. 2014; ready to take beam 5000 hr., Feb-Dec 2015

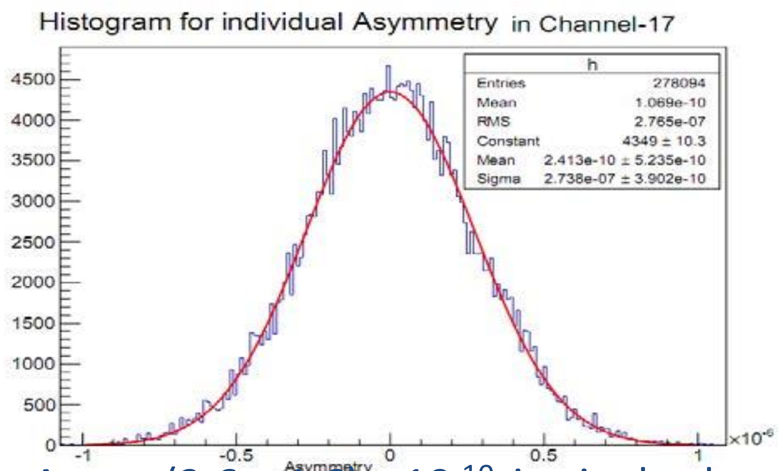

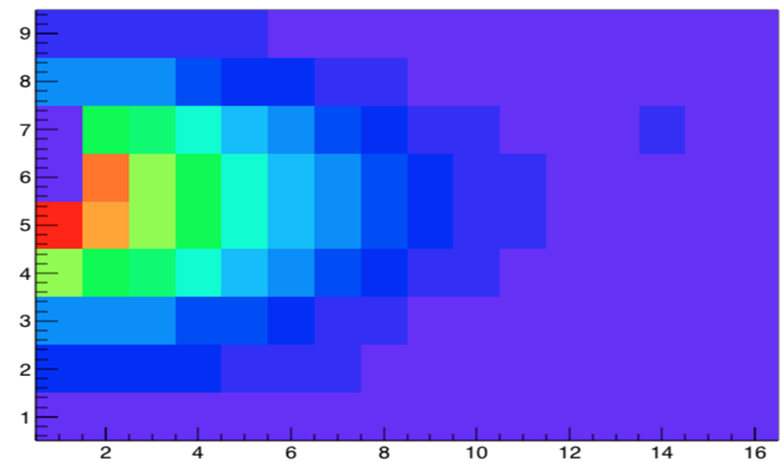

A_{instr} = (2.6 ± 1.6) x 10^{-10} in single chanel

Ionization current in each cell

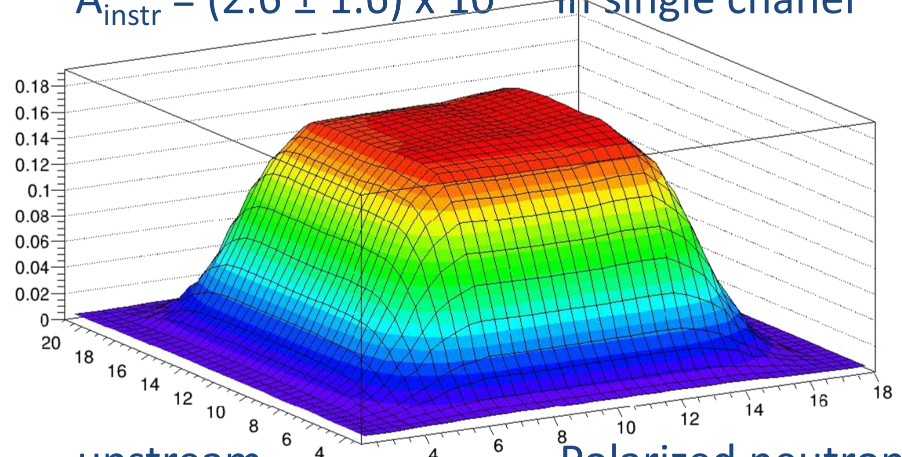

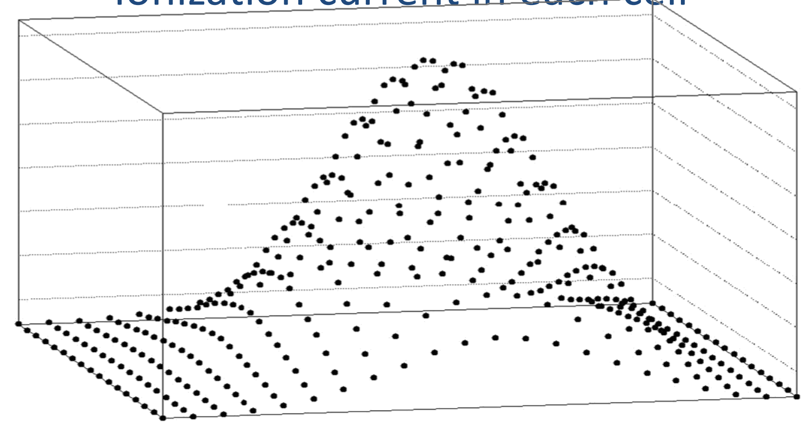

upstream Polarized neutron spatial profile downstream

Asymmetry Measurement – Statistics

- PV physics asymmetry
  - Extracted from weighted average of single-wire spin asymmetries
  - Sensitivities calculated by MC
- 15% measurement in 1 beam c

$$\delta A = \frac{\sigma_d}{P\sqrt{N}} = 1.6 \times 10^{-8}$$

$N = 1.5\times10^{10}$ n/s $\times 10^{7}$ s (116 days)

$P = 96.2\%$ neutron polarization

$\sigma_d = 6$ detector inefficiency

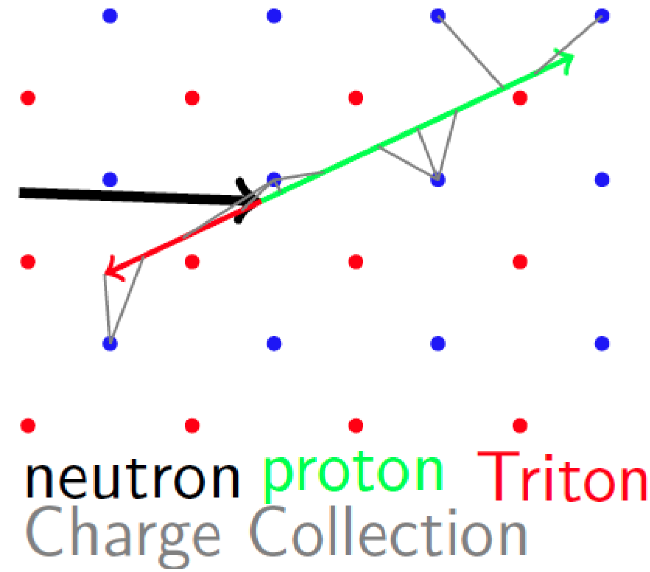

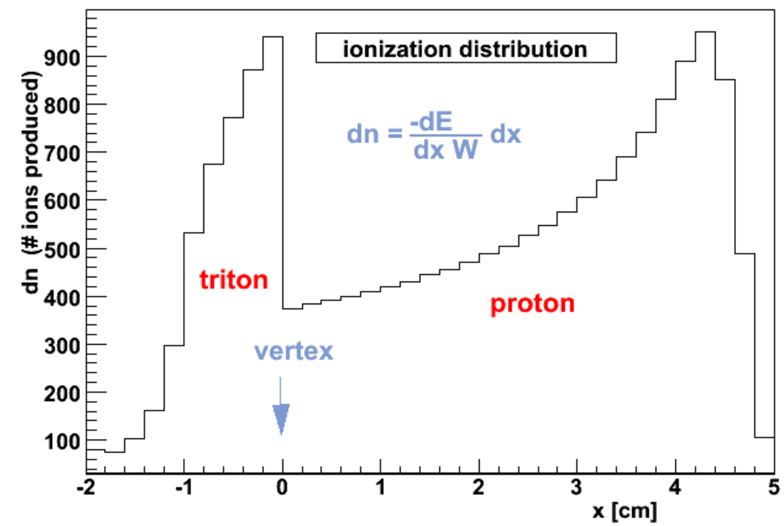

UK UNIVERSITY OF KENTUCKY

Systematic Uncertainties

- Beam fluctuations, polarization, RFSF efficiency: $$A_{exp} = \frac{A_b + PA}{1 + A_p PA}$$
- $k_n r \sim 10^{-5}$ small for cold neutrons
- PC asymmetries minimized with longitudinal polarization
- Alignment of field, beam, and chamber to 10 mrad is achievable
- Unlike n p –> d ° or n d –> t °,
  n-^{3}He is very insensitive to gammas (only Compton electrons)

Invariant	Parity	Size	Comments
$\vec{\sigma}_n \cdot \vec{k}_p$	Odd	3×10^{-7}	Nuclear capture asymmetry
$\vec{\sigma}_n \cdot (\vec{k}_n \times \vec{k}_p)$	Even	2×10^{-10}	Nuclear capture asymmetry
	Even	6×10^{-12}	Mott-Schwinger scattering
$\vec{\sigma}_n \cdot \vec{B}$	Even	1×10^{-10}	Stern-Gerlach steering
	Even	2×10^{-11}	Boltzmann polarization of ^{3}He
	Even	4×10^{-13}	Neutron induced polarization of ^{3}He
$\vec{\boldsymbol{\sigma}}_n \cdot \vec{k}_p$	Odd	1×10^{-11}	Neutron beta decay

$A_P^{\vec{n}^3He}$

Conclusion

- Hadronic Parity Violation
  - Is a complementary probe of nuclear and nucleonic structure
  - Need 4 experiments to isolate spin and isospin dependence
  - With pp (45MeV), pp (220 MeV), NPDGamma, n-3He, NSR-III we can test the self-consistency of HWI formalisms
- NPDGamma Experiment
  - Sensitive to long-range coupling $f_{¼}$
  - Results to be released soon
- n-^{3}He Experiment
  - 15% projected uncertainty: most accurate few-body HWI experiment
  - FnPB beam: June 2014 – Dec 2015

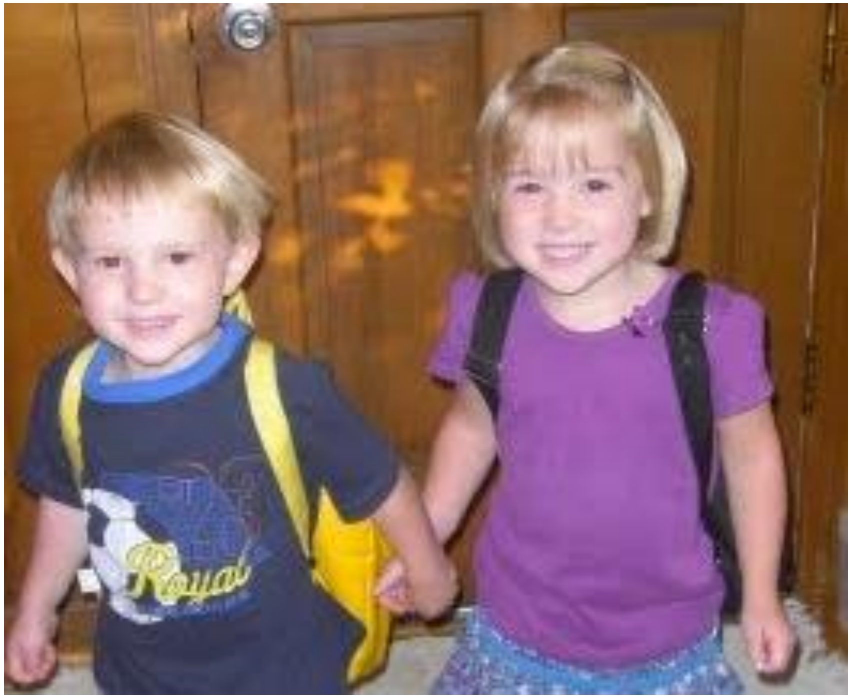

Thank you!